

Taking Care of The Discretization Problem: A Black-Box Adversarial Image Attack in Discrete Integer Domain

Yuchao Duan
Nanjing University

Zhe Zhao
ShanghaiTech University

Lei Bu
Nanjing University

Fu Song
ShanghaiTech University

Abstract—Numerous adversarial attacks on neural network based classifiers have been proposed recently with high success rate. Neural network based image classifiers usually normalize valid images into some real continuous domain and make classification decisions on the normalized images using the neural networks. However, existing attacks often craft adversarial examples in such domain, which may become benign once denormalized back into the discrete integer domain, known as the discretization problem. This problem has been mentioned in some work, but has received relatively little attention.

To understand the impacts of the discretization problem, in this work, we report the first comprehensive study of existing works. We theoretically analyze 35 representative methods and empirically study 20 representative open source tools for crafting adversarial images. We found 29/35 (theoretically) and 14/20 (empirically), are affected, e.g., the success rate could dramatically drop from 100% to 10%. This reveals that the discretization problem is far more serious than originally thought and suggests that it should be taken into account seriously when crafting adversarial examples and measuring attack success rate.

As a first step towards addressing this problem in black-box scenario, we propose a novel method which directly crafts adversarial examples in discrete integer domains. Our method reduces adversarial attack problem to a derivative-free optimization (DFO) problem for which we propose a classification model-based DFO algorithm. Experimental results show that our method achieves close to 100% attack success rates for both targeted and untargeted attacks, comparable to the most popular white-box methods (FGSM, BIM and C&W), and significantly outperforms representative black-box methods (ZOO, AutoZOOM, NES-PGD, Bandits, FD, FD-PSO and GenAttack). Moreover, our method successfully breaks the winner of NIPS 2017 competition on defense with 100% success rate. Our results suggest that discrete optimization algorithms open up a promising area of research into effective black-box attacks.

Index Terms—Adversarial examples, deep neural networks, discretization, black-box attacks, derivative-free optimization

I. INTRODUCTION

In the past 10 years, machine learning algorithms, fueled by massive amounts of data, achieve human-level performance or better on a number of tasks. Models produced by machine learning algorithms, especially deep neural networks, are increasingly being deployed in a variety of applications such as autonomous driving [1]–[3], medical diagnostics [4]–[6], robotics [7], [8], and cyber-security [9]–[11].

In the early stage of machine learning, people pay more attention to the basic theory and application research, although it is known in 2004 that machine learning models

are often vulnerable to adversarial manipulation of their input intended to cause misclassification [12]. In 2014, Szegedy et al. proposed the concept of adversarial examples for the first time in deep neural network setting [13]. By adding a subtle perturbation to the input of the deep neural network, it results in a misclassification. Since these findings, a plethora of studies have shown that the state-of-the-art deep neural networks suffer from the adversarial example attacks which can lead to severe consequences when applied to real-world applications [14]–[37]. In the literature, there are mainly two types of complementary techniques: testing based [13], [16], [21]–[24], [28], [29], [31]–[38] and verification based [22], [36], [39]–[44] methods for crafting adversarial examples.

However, almost all existing adversarial example attacks target neural networks rather than neural network based classifiers, while neural network based classifiers differ from neural networks. As a matter of fact, in image classification setting, valid images in computer systems are stored in some format (e.g., png and jpeg) formed as a discrete integer domain (e.g., $\{0, \dots, 255\}^m$), but will be normalized into some continuous real domain (e.g., $[0, 1]^m$) for training and testing neural network models [45]. Therefore, a neural network based image classifier consists of a pre-processor for normalization and a neural network model. As a result, adversarial examples crafted by existing attacks against neural networks are in the continuous real domain. Such adversarial examples do fool the target neural network, but once denormalized back into the discrete integer domain as valid images, may become benign for the neural network based image classifier. This gap was initially considered by Goodfellow et al. [15] and Papernot et al. [19], and latter formally presented by Carlini and Wagner, called *the discretization problem* [18]. Carlini and Wagner stated that “*This rounding will slightly degrade the quality of the adversarial example*” according to their experimental results on MNIST images. Later on, this problem has received relatively little attention. We believe, there lacks a comprehensive study on the impacts of the discretization problem: e.g., which methods/tools may be affected, to what extent does this problem affect the attack success rate and can it be avoided or alleviated?

To understand the impacts of the discretization problem, in this work, we report the first comprehensive study of existing works for crafting adversarial examples in image classification

domain which has a plethora of studies. In the rest of this work, adversarial examples in a continuous real domain will be called *real* adversarial examples and adversarial examples in a discrete integer domain will be called *integer* adversarial examples.

We theoretically analyze 35 representative methods for crafting adversarial examples. We find that:

- Almost all of them craft real adversarial examples;
- 29 methods are affected by the discretization problem;
- 23 works do not provide hyper-parameters so that the discretization problem could not be easily and directly avoided.

To understand the impacts of the discretization problem in practice, we carry out an empirical evaluation of 20 representative open source tools. We evaluate the gap between the attack success rates of crafted real adversarial examples and their corresponding integer adversarial examples. Our empirical study shows that:

- Most of the 20 tools are affected by the discretization problem. In our experiments, there are 8 tools whose gap exceeds 50%, 6 tools whose gap exceeds 70%, and only 6 tools do not have any gaps.
- Among the 14 tools that are affected by the discretization problem, only 1 tool (FGSM) can avoid the discretization problem by tuning input parameters, 3 tools can alleviate the discretization problem by tuning input parameters at the cost of attack efficiency or imperceptibility of adversarial examples, and 10 tools can neither avoid nor alleviate the discretization problem by tuning input parameters.

Our study reveals that the discretization problem is far more serious than originally thought and suggests to take it into account seriously when crafting digital adversarial examples and measuring attack success rate.

According to our comprehensive study, we found there lacks an effective and efficient integer adversarial example attack in black-box scenario. As the second main contribution of this work, we propose a black-box algorithm that directly crafts adversarial examples in discrete integer domains for both targeted and untargeted attacks. Our method only requires access to the probability distribution of classes for each test input. We formalize the computation of integer adversarial examples as a black-box discrete optimization problem constrained with a \mathbb{L}_∞ distance, where \mathbb{L}_∞ is defined in the discrete domain as well. However, this discrete optimization problem cannot be solved using gradient-based methods, as the model is non-continuous. To solve this problem, we propose a novel classification model-based derivative-free discrete optimization method that does not rely on the gradient of the objective function, but instead, *learns* from samples of the search space and *refines* the search space into small subspaces. It is suitable for optimizing functions that are non-differentiable, with many local minima, or even unknown but only testable.

We demonstrate the effectiveness and efficiency of our method on the MNIST dataset [46] using the LeNet-1 model [47]; and the ImageNet dataset [48] using Inception-v3 [49] model. Our method achieves close to 100% attack success rates for both targeted and untargeted attacks, comparable to the state-of-the-art white-box attacks: FGSM [15], BIM [23] and C&W [18], and significantly outperforms representative black-box methods: ZOO [30], AutoZOOM [34], NES-PGD [37], Bandits [50], GenAttack [51], substitute model based black-box attacks with FGSM and C&W methods, FD and FD-PSO [52]. In terms of query efficiency, our attack is comparable to (or better than) the black-box attacks: NES-PGD, Bandits, AutoZOOM, and GenAttack, which are specially designed for query-limited scenarios. Moreover, our method is able to break the HGD defense [53], which won the first place of NIPS 2017 competition on defense against adversarial attacks, with 100% success rate, and also achieves the so-far best success rate of white-box attacks in the online MNIST Adversarial Examples Challenge [54].

Our contributions in this paper include:

- We report the first comprehensive study of existing works on the discretization problem, including 35 representative methods and 20 representative open source tools.
- Our study sheds light on the impacts of the discretization problem, which is useful to the community.
- We propose a black-box algorithm for crafting integer adversarial examples for targeted/untargeted attacks by designing a derivative-free discrete optimization method.
- Our attack achieves close to 100% attack success rate, comparable to several recent popular white-box attacks, and outperforms several recent popular black-box tools (e.g., ZOO, Bandits, AutoZOOM, GenAttack and NES-PGD) in terms of integer adversarial examples.
- Our attack is able to break the HGD defense [53] with 100% success rate, and also achieves the same result as the best white-box attack in MNIST Challenge [54].

To the best of our knowledge, this is the first comprehensive study of the impacts of the discretization problem on adversarial examples and the first black-box attack that directly crafts adversarial examples in discrete integer domain.

II. RELATED WORK

Digital adversarial attacks in white-box scenario have been widely studied in the literature, to cite a few [13], [16], [21], [22], [22], [28], [29], [38]–[43]. In white-box scenario, the adversary has access to details (e.g., architecture, parameters, training dataset) of the system under attack. This setting is clearly impractical in real-world cases, when the adversary cannot get access to the details. Therefore, in this work, we propose black-box adversarial attacks. In the rest of this section, we mainly discuss existing works on black-box adversarial attacks .

A. Digital Adversarial Attack

We classify existing attack methods along three dimensions: substitute model, gradient estimation and heuristic search.

Substitute Model. Papernot et al. [32] proposed the first black-box method by leveraging transferability property of adversarial examples. It first trains a local substitute model with a synthetic dataset and then crafts adversarial examples from the local substitute model. [55] generalized this idea to attack other machine learning classifiers. However, transferability is not always reliable, other methods such as gradient estimation are explored as alternatives to substitute networks.

Gradient Estimation. Gradient plays an important role in white-box adversarial attacks. Therefore, estimating the gradient to guide the search of adversarial examples is a popular research direction in black-box adversarial attacks. Chen et al. [30] proposed a black-box attack method (named ZOO) with zeroth order optimization. Following ZOO, Tu et al. [34] proposed an autoencoder-based method (named AutoZOOM) to improve query efficiency. Similarly, Bhagoji et al. [52] proposed a class of black-box attacks (called FD) that approximate FGSM and BIM via gradient estimation. Independently, Ilyas et al. [37] proposed an alternative gradient estimation method by leveraging natural evolution strategy (NES) [56], [57] and employing white-box PGD attack with estimated gradient (named NES-PGD). Based on NES-PGS, Ilyas et al. [50] proposed a bandit optimization-based method aimed at enhancing query efficiency. Recently, Zhao et al. [58] proposed a method to leverage an alternating direction method of multipliers (ADMM) algorithm for gradient estimation.

Heuristic Search. Instead of gradient estimation, heuristic search-based derivative-free optimization (DFO) methods have been proposed. Brendel et al. [24] proposed a decision-based attack (named DBA) with label-only setting, which starts from the target image, moves a small step to raw image every time and checks the perturbation cross the decision boundary or not. Su et al. [59] proposed a black-box attack for generating one-pixel adversarial images based on differential evolution. Bhagoji et al. [52] also proposed a particle swarm optimization (PSO) based DFO method, named FD-PSO. PSO previously was used to find adversarial examples to fool face recognition systems [20]. In a concurrent work, Alzantot et al. [51] proposed a genetic algorithm based DFO method (named GenAttack) for generating adversarial images. Genetic algorithm was previously used to find adversarial examples to fool pdf malware classifiers in EvadeML [60]. Co et al. [61] proposed a method for generating universal adversarial perturbations (UAPs) in the black-box attack scenario by leveraging Bayesian optimization, it is a new interesting area to generate procedural noise perturbations.

Different from the above heuristic search based methods, we present a classification model-based DFO method, to distinguish “good” samples with “bad” samples. By learning from the evaluation of the samples, our algorithm iteratively refines large search space into small-subspaces, finally converges to the best solution. Experimental results show that our method achieves significantly higher success rate in terms of the integer adversarial examples than the state-of-the-art tools from all the above classes, with comparable query times (cf.

Section VI).

B. Physical Adversarial Attack

Thanks to the success of adversarial example attacks in the digital domain, recently, researchers started to study the feasibility of adversarial examples in the physical world. We now discuss recent efforts on physical adversarial examples.

Kurakin showed that printed adversarial examples crafted in the digital domain can be misclassified when viewed through a smartphone camera [23]. Follow-up works proposed methods to improve robustness of physical adversarial examples by synthesizing the digital images to simulate the effect of rotation, brightness and scaling, and digital-to-physical transformation [28], [29], [62], [63], or manually taking physical photos from different viewpoints and distances [28], [64], or adding scene-independent patch [65]. Furthermore, adversarial example attacks have been applied on road sign images [66], [67], face recognition systems [20] and object detectors [68], [69]. Physical adversarial examples that are printed or showed by devices will not be affected by the discretization problem.

Although, these works demonstrated that physical adversarial examples are possible, it is still very useful to generate effective integer adversarial images.

- First, it can be used in many practical scenarios, e.g., attacking the online image classification systems.
- Second, an attacker who cannot fool a classifier successfully in the digital domain will also struggle to do so physically in practice [20].
- Third, it usually requires relatively expensive manual efforts to directly craft physical adversarial examples. On the other hand, robust digital adversarial examples can survive in physical world [63].

It is interesting to study the impacts of the discretization problem on the difficulty of finding physical adversarial examples. To apply our classification model-based derivative free optimization method on physical attack is also an interesting topic. We leave these topics to future work.

C. Other Attacks

Adversarial example attacks against other machine learning based classifiers also have been exhibited, such as malicious PDF files [60], [70], [71], malware [72], [73], malicious websites [74], spam emails [75], and speech recognition [76], [77]. Since each type of machine learning based classifiers has unique characteristics, in general, these existing attacks are orthogonal to our work.

III. BACKGROUND

In this section, we introduce deep learning based image classifications, adversarial attacks and distance metrics. For convenient reference, we summarize the notations in Table I.

A. Deep Learning based Image Classification

Valid images are represented as integer images in computer systems. To train a practical image classifier $f_t : \mathbb{D} \rightarrow \mathbb{C}_t$, valid images should first be normalized so that their pixels all

TABLE I
NOTATIONS USED IN THIS PAPER

Notation	Description
w, h, ch	width, height, and number of channels of an image
P	the set of coordinates $w \times h \times ch$
\mathbb{V}	continuous (real) domain of real images \vec{v} , e.g., $\mathbb{R}_{[0,1]}^{w \times h \times ch}$
\mathbb{D}	discrete (integer) domain of integer images \vec{d} , e.g., $\mathbb{N}_{[0,255]}^{w \times h \times ch}$
$\vec{v}, \vec{v}^{\text{adv}} \in \mathbb{V}$	continuous real (adversarial) image
$\vec{d}, \vec{d}^{\text{adv}} \in \mathbb{D}$	discrete integer (adversarial) image
$\vec{v}[p]$	entity at coordinate p of a real image \vec{v}
$\vec{d}[p]$	entity at coordinate p of an integer image $\vec{d} \in \mathbb{D}$
$\mathbb{T} : \mathbb{D} \rightarrow \mathbb{V}$	normalizer that transforms an integer image into a real image in the continuous domain \mathbb{V}
$\mathbb{T}^{-1} : \mathbb{V} \rightarrow \mathbb{D}$	denormalizer that transforms a real image back into an integer image such that $\forall \vec{d} \in \mathbb{D}, \mathbb{T}^{-1}(\mathbb{T}(\vec{d})) = \vec{d}$
\mathbb{C}_t	set of mutually exclusive classes for the task t

lie in the same reasonable range, as integer images come in a form that is difficult for many deep learning architectures to represent [45]. Therefore, as shown in Figure 1, the classifier f_t is constructed by training an image classifier $g_t : \mathbb{V} \rightarrow \mathbb{C}_t$ in continuous (real) domain aided by a normalizer $\mathbb{T} : \mathbb{D} \rightarrow \mathbb{V}$, which leads to the classifier $f_t = g_t \circ \mathbb{T}$.

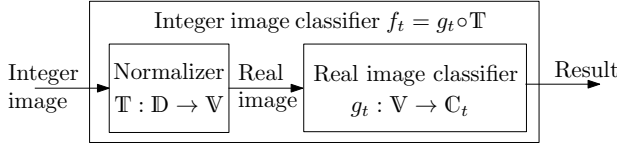


Fig. 1. Overview of machine learning based image classifiers.

B. Adversarial Attacks

In this work, we consider adversarial attacks using digital adversarial examples instead of physical adversarial examples. We categorize digital adversarial examples into *real* and *integer* ones according to their domains \mathbb{V} and \mathbb{D} .

Real and integer adversarial examples. A *real adversarial example* crafted from a real image $\vec{v} \in \mathbb{V}$ is an image $\vec{v}^{\text{adv}} \in \mathbb{V}$ such that the real image classifier g_t misclassifies \vec{v}^{adv} , i.e., $g_t(\vec{v}) \neq g_t(\vec{v}^{\text{adv}})$. Likewise, an *integer adversarial example* crafted from an integer image $\vec{d} \in \mathbb{D}$ is an image $\vec{d}^{\text{adv}} \in \mathbb{D}$ such that the integer image classifier f_t misclassifies \vec{d}^{adv} , i.e., $f_t(\vec{d}) \neq f_t(\vec{d}^{\text{adv}})$.

Untargeted and targeted attacks. In the literature, there are two types of adversarial attacks: targeted and untargeted attacks. Untargeted attack aims at crafting an adversarial example that misleads the system being attacked, i.e., $g_t(\vec{v}) \neq g_t(\vec{v}^{\text{adv}})$ for real adversarial examples and $f_t(\vec{d}) \neq f_t(\vec{d}^{\text{adv}})$ for integer adversarial examples. A more powerful but difficult attack, targeted attack, aims at crafting an adversarial example such that the system classifies the adversarial example as the given class c , i.e., $g_t(\vec{v}^{\text{adv}}) = c$ for real adversarial examples and $f_t(\vec{d}^{\text{adv}}) = c$ for integer adversarial examples. It is easy

to see that targeted attack can be used to launch untargeted attack by choosing an arbitrary target class.

White-box and black-box scenarios. Targeted and untargeted attacks have been studied in both white-box and black-box scenarios, according to the knowledge of the target system. In white-box scenario, the adversary has access to details (e.g., architecture, parameters and training dataset) of the system under attack. This setting is clearly impractical in real-world cases, when the adversary cannot get access to the details. In a more realistic black-box scenario, it is usually assumed that the adversary can only query the system and obtain confidences or probabilities of classes for each input by limited queries.

In black-box scenario, we emphasize that the adversary has no access to the normalization of the target classification system, otherwise the attack would be a gray-box one. It is also non-trivial to infer the normalization by the adversary in black-box scenario due to the diversity of normalization. Indeed, there is no standard normalization in literature and they may differ in tools, neural network models and datasets. For instance, let i denote the integer value of a coordinate,

- the Inception-v3 model on ImageNet dataset in ZOO [30] uses the normalization: $v_1 = (i/255 - 0.5)$;
- the Inception-v3 model on ImageNet dataset in Keras [78] uses the normalization: $v_2 = ((2 \times i)/255 - 1)$;
- the VGG and ResNet models on ImageNet dataset in Keras [78] use the normalization: $v_3 = (i - mean)$, where *mean* denotes the mean value of images in training dataset.

To the best of our knowledge, there is no work on inferring normalization of classifiers. More details refer to Appendix A.

C. Distance Metrics

The distortion of adversarial examples should be visually indistinguishable from their normal counterparts by humans. However, it is hard to model human perception, hence several distance metrics were proposed to approximate human's perception of visual difference. In the literature, there are four common distance metrics \mathbf{L}_0 , \mathbf{L}_1 , \mathbf{L}_2 and \mathbf{L}_∞ which are defined over samples in some continuous domain \mathbb{V} . All of them are \mathbf{L}_n norm defined as

$$\|\vec{v} - \vec{v}^{\text{adv}}\|_n = \left(\sum_{p \in P} |\vec{v}[p] - \vec{v}^{\text{adv}}[p]|^n \right)^{\frac{1}{n}},$$

where $\vec{v}, \vec{v}^{\text{adv}} \in \mathbb{V}$. In more detail, \mathbf{L}_0 counts the number of different coordinates, i.e., $\sum_{p \in P} (\vec{v}[p] \neq \vec{v}^{\text{adv}}[p])$; \mathbf{L}_1 denotes the sum of absolute differences of each coordinate value, i.e., $\sum_{p \in P} (|\vec{v}[p] - \vec{v}^{\text{adv}}[p]|)$; \mathbf{L}_2 denotes Euclidean or root-mean-square distance; and \mathbf{L}_∞ measures the largest change introduced. Remark that

$$\lim_{n \rightarrow \infty} \|\vec{v} - \vec{v}^{\text{adv}}\|_n = \max\{|\vec{v}[p] - \vec{v}^{\text{adv}}[p]| \mid p \in P\}.$$

However, it seems not reasonable to approximate human's perception of visual difference using distance metrics defined between real images. Instead, it is much better to measure the distance between integer images. For this purpose, we

revise distance metrics and introduce \mathbb{L}_p norm which is defined between integer images. Formally, \mathbb{L}_n is defined as follows:

$$\|\vec{d} - \vec{d}^{\text{adv}}\|_n = \left(\sum_{p \in P} \left| \vec{d}[p] - \vec{d}^{\text{adv}}[p] \right|^n \right)^{\frac{1}{n}},$$

where $\vec{d}, \vec{d}^{\text{adv}} \in \mathbb{D}$. Accordingly, we define: $\mathbb{L}_0 = \|\vec{d} - \vec{d}^{\text{adv}}\|_0$, $\mathbb{L}_1 = \|\vec{d} - \vec{d}^{\text{adv}}\|_1$, $\mathbb{L}_2 = \|\vec{d} - \vec{d}^{\text{adv}}\|_2$ and $\mathbb{L}_\infty = \|\vec{d} - \vec{d}^{\text{adv}}\|_\infty$. Obviously, \mathbb{L}_n differs from \mathbb{L}_n for any n .

IV. THE DISCRETIZATION PROBLEM

Recall that we categorize digital adversarial examples into real and integer ones according to their domains. There is a gap between adversarial examples in continuous and in discrete domains. In this section, we first formalize the gap as the discretization problem and then report the comprehensively study of the impacts of the discretization problem.

A. Formulation of The Discretization Problem

Recall that a practical image classification system f_t is an integer image classifier that consists of both the real image classifier g_t and the normalizer \mathbb{T} . Therefore, to attack the system f_t using a real adversarial image $\vec{v}^{\text{adv}} \in \mathbb{V}$ that is crafted by querying g_t , it is necessary to denormalize the real image \vec{v}^{adv} back into a valid image (i.e, an integer image) $\vec{d}^{\text{adv}} \in \mathbb{D}$, so that it can be fed to the target system f_t . To denormalize \vec{v}^{adv} , a denormalizer \mathbb{T}^{-1} should be implemented according to the knowledge of the normalizer \mathbb{T} such that for any integer image $\vec{d} \in \mathbb{D}$, $\mathbb{T}^{-1}(\mathbb{T}(\vec{d})) = \vec{d}$.

However, after applying the denormalization, \vec{d}^{adv} may be classified as a class that differs from the one of \vec{v}^{adv} , i.e.,

$$f_t(\vec{d}^{\text{adv}}) = f_t(\mathbb{T}^{-1}(\vec{v}^{\text{adv}})) = g_t(\mathbb{T}(\mathbb{T}^{-1}(\vec{v}^{\text{adv}}))) \neq g_t(\vec{v}^{\text{adv}}).$$

This is so-called *the discretization problem*¹, which comes from the non-equivalent transformation between continuous real and discrete integer domains, i.e., $\mathbb{T}(\mathbb{T}^{-1}(\vec{v}^{\text{adv}})) \neq \vec{v}^{\text{adv}}$, resulting in

$$g_t(\mathbb{T}(\mathbb{T}^{-1}(\vec{v}^{\text{adv}}))) \neq g_t(\vec{v}^{\text{adv}}).$$

In the rest of this work, the maximum error when transforming a real adversarial image back into the discrete domain is called *discretization error*.

The discretization problem may result in failure of untargeted and targeted attacks, i.e.,

$$f_t(\mathbb{T}^{-1}(\vec{v}^{\text{adv}})) = f_t(\vec{d}) \text{ or } f_t(\mathbb{T}^{-1}(\vec{v}^{\text{adv}})) \neq c.$$

where \vec{v}^{adv} denotes a real adversarial image crafted from $\mathbb{T}(\vec{d})$ and c denotes the target class.

As stated by Carlini and Wanger [18], the discretization problem slightly degrades the quality of the adversarial example. However, there lacks a comprehensive study of the impacts of the discretization problem. In the rest of this section, we report the first comprehensive study including theoretically analysis of 35 representative methods and empirically study

¹The term ‘‘discretization’’ comes from Carlini and Wagner [18] which expresses the rounding problem from real numbers to integer numbers. Our definition is more general than theirs.

TABLE II
SUMMARY OF THEORETICAL STUDY RESULTS

	Reference	(Un)targeted	Domain	Considered	B2G	Avoidable	
Testing-based methods	White-box	L-BFGS [13]	Targeted	Continuous	✗	-	✗
		FGSM [15]	Untargeted	Continuous	✓	-	✓
		BIM(ILLC) [23]	Targeted	Discrete	-	-	-
		PGD [79]	Untargeted	Continuous	✗	-	✗
		MBIM [80]	Targeted	Continuous	✗	-	✓
		J SMA [19]	Targeted	Continuous	✗	-	✓
		C&W [18]	Targeted	Continuous	✓	-	✗
		OptMargin [81]	Untargeted	Continuous	✗	-	✗
		EAD [82]	Targeted	Continuous	✗	-	✗
		DeepFool [83]	Untargeted	Continuous	✗	-	✗
	UAP [21]	Untargeted	Continuous	✗	-	✗	
	DeepXplore [22]	Untargeted	Continuous	✗	-	✗	
	DeepCover [84]	Untargeted	Continuous	✗	-	✗	
	DeepGauge [38]	Untargeted	Continuous	✗	-	-	
	DeepConcolic [85]	Untargeted	Continuous	✓	-	✗	
	Black-box	SModel [32]	Targeted	Continuous	✗	✗	-
		PMG [55]	Untargeted	Continuous	✗	✗	-
		One-pixel [59]	Targeted	Continuous	✗	✗	✗
		ZOO [30]	Targeted	Continuous	✗	✓	✗
		FD [52]	Targeted	Continuous	✗	✗	-
NES-PGD [37]		Targeted	Continuous	✗	✗	✗	
DBA [24]		Targeted	Continuous	✗	✗	✗	
Bandits [50]		Untargeted	Continuous	✗	✗	✗	
AutoZOOM [34]		Targeted	Continuous	✗	✓	✗	
GenAttack [51]		Targeted	Continuous	✗	✓	✗	
Verification methods	White-box	Reference	Complete	Domain	Considered	B2G	Avoidable
		BILVNC [86]	✓ → ✗	Continuous	✗	-	✗
		DLV [87]	✗	Continuous	✓	-	✓
		Planet [88]	✓ → ✗	Continuous	✗	-	✗
		MIPVerify [89]	✓ → ✗	Continuous	✗	-	✗
		DeepZ [43]	✗	Continuous	✗	-	✗
		DeepPoly [44]	✗	Continuous	✗	-	✗
		DeepGo [90]	✗	Continuous	✗	-	✗
		ReluVal [91]	✓ → ✗	Continuous	✗	-	✗
	DSGMK [92]	✓ → ✗	Continuous	✗	-	✗	
B	SafeCV [36]	✗	Continuous	✓	✓	✓	

Note: These results are summarized mainly according to their raw papers and source code. (Un)targeted column shows the type of attack, once a method could launch targeted attack, we mark it as targeted, as targeted is more powerful than untargeted attack; Domain column shows the domain of images; Considered column shows whether the method considered the discretization problem; B2G column shows whether black-box downgrades to gray-box; Avoidable column shows whether the discretization problem could be (almost) avoided; Complete column shows whether the method is complete, → meaning complete method becomes incomplete due to the discretization problem.

of 20 representative open source tools, in an attempt to understand the impacts of the discretization problem.

B. Theoretical Study

We theoretically analyze 35 existing works including 25 testing methods (15 white-box and 10 black-box) and 10 verification methods (9 white-box and 1 black-box), to determine: 1) whether they generate adversarial examples in discrete or continuous domain? 2) if they use some continuous domain, do they consider the discretization problem and how do they deal with? and 3) if they do not consider, could the discretization problem be avoided by tuning input parameters? The summary of results is given in Table II according to raw papers (primarily) and source code.

Discrete or continuous. After examining the domain of all the 35 works, we found only BIM defines the adversarial example searching problem in discrete domains and uses the integer perturbation step sizes. While the other 34 works craft adversarial examples in continuous domains, hence they may be affected by the discretization problem.

Considered or not. Among 34 works that craft adversarial example in continuous domains, we found only five works (i.e., FGSM, C&W, DeepConcolic, DLV and SafeCV) do consider the discretization problem, while the other 29 works do not, indicating that 29 out of 35 works are affected by the discretization problem.

Specifically, FGSM uses perturbation step sizes that correspond to the magnitude of the smallest bit of an image so that the transformation between continuous and discrete domains are almost equivalent, i.e., the discretization errors are nearly zero. DLV verifies classifiers by means of discretization such that the crafted real adversarial examples are still adversarial after denormalization. SafeCV limits the perturbation of each pixel to the minimum or maximum values of coordinates. Therefore, the discretization problem in FGSM, DLV and SafeCV are (almost) avoided.

In contrast, C&W and DeepConcolic perform denormalization post-processing before checking crafted real images, and C&W also proposes a greedy algorithm that searches integer adversarial examples on a lattice defined by the discrete solutions by changing one pixel value at a time. However, discrete solutions are computed by rounding real numbers of coordinates in real adversarial examples to the nearest integers. Therefore, DeepConcolic and C&W either evade or alleviate the discretization problem, but they *cannot* essentially avoid it in theory, as they may craft many useless real adversarial examples.

Avoidable or not. We further conduct an in-depth analysis of 29 works that craft adversarial example in continuous domains, but do not consider the discretization problem. We investigate whether the discretization problem in these works can be easily and directly avoided by tuning hyper-parameters. We found that only MBIM and JSMA could control the perturbation step sizes directly by hyper-parameters so that the discretization problem could be (almost) avoided by choosing proper perturbation step sizes.

In contrast, 23 out of 29 works do not provide such hyper-parameters so that the discretization problem could not be easily and directly avoided. This is because that

- PGD, DeepXplore, One-pixel, NES-PGD, DBA, Bandits and GenAttack introduce random perturbation step size or random noise, making perturbation step size uncontrollable;
- L-BFGS, OptMargin, EAD, DeepFool, DeepCover, UAP, ZOO and AutoZOOM directly craft perturbations (e.g., from optimizers) in continuous domain;
- BILVNC, Planet, MIPVerify, DeepZ, DeepPoly, DeepGo, ReluVal, and DSGMK do not provide any parameters to constrain real adversarial examples so that the discretization error cannot be minimized.

The remaining 4 methods DeepGauge, SModel, PMG and FD actually leverage other attack methods such as (FGSM, BIM, JSMA, and C&W). Therefore, the impacts of the discretization problem on their methods rely upon other attacks.

Discussion. After an in-depth analysis of 35 existing works, we found that 34 works craft adversarial example in continuous domains, 29 works are affected by the discretization problem, and 23 works do not provide hyper-parameters to avoid the discretization problem. As aforementioned, real adversarial examples may be damaged when transform them back into valid images, due to the discretization problem, hence fail to launch attacks. Besides this, there are other severe consequences: (1) the black-box methods such as ZOO, AutoZOOM, GenAttack and SafeCV downgrade to gray-box ones, as they directly invoke the normalization of the integer classification systems; (2) the verification methods such as BILVNC, MIPVerify, Planet and ReluVal that are claimed complete are only limited to real image classifiers, and become incomplete on practical image classification systems that are indeed integer image classifiers; and (3) the verification methods such as BILVNC, MIPVerify, Planet, ReluVal, DeepZ, DeepPoly, DeepGo and DSGMK may craft spurious adversarial examples and fail to prove robustness of integer image classifiers.

Moreover, during our study, we found there are lots of Github issues, e.g., [93]–[95], asking why adversarial examples are damaged after saving. Users might doubt whether implementations are correct or images are saved in a correct way. According to our findings, it is due to the discretization problem.

C. Empirical Study

We conduct an empirical study on 20 representative methods in Table III whose source code is publicly available, in an attempt to understand the impacts of the discretization problem in practice.

We consider the following two research questions:

RQ1: To what extent does the discretization problem affect the attack success rate?

RQ2: Can the discretization problem be avoided or alleviated by tuning input parameters?

Setting. In our experiments, we use the official implementations of the authors. Due to the diversity of these tools, the dataset and setting may be different. We manage to be consistent with the original environments in their raw papers, attack the target models provided by the tools, and conduct targeted attacks unless the tools are designated for untargeted attacks. For verification tools that cannot directly attack the model, we evaluate them by analyzing the generated counterexamples. Although, we do not change their settings deliberately to get exaggerative results, we should emphasize that the comparison between these tools may be unfair, *our main goal is to understand their own tools.*

Dataset. We use two popular image datasets: MNIST [46] and ImageNet [48]. ImageNet contains over 10000000 images with 1000 classes. We randomly choose 100 classes from which we randomly choose 1 image per class that can be correctly classified by four classifiers in Keras: ResNet50, Inception-v3, VGG16 and VGG19. For MNIST images, the numbers of

TABLE III
EXPERIMENT RESULTS ON THE DISCRETIZATION PROBLEM

Method	SR	TSR	GAP	Dataset	Model	Default	Note
FGSM [15]	98.61%	98.58%	0.03%	MNIST	LeNet-1 [‡]	✓	10000 images
BIM [23]	100%	100%	0%	ImageNet	Inception-v3 [‡]	✓	-
MBIM [80]	100%	100%	0%	ImageNet	Inception-v3 [‡]	✓	-
JSMA [19]	96%	96%	0%	ImageNet	VGG19 [‡]	✓	-
L-BFGS [96]	100%	77%	23%	ImageNet	Inception-v3 [‡]	✓	-
C&W-L ₂ [18]	100%	10%	90%	ImageNet	Inception-v3*	✓	-
DeepFool [83]	100%	23%	77%	ImageNet	ResNet34*	✓	-
DeepXplore [22]	65%	28%	56.92%	ImageNet	ResNet50, VGG16&19*	✓	Generate examples with 100 seeds
DeepConcolic [85]	2%	2%	0%	MNIST	mnist_complicated.h5*	✓	10000 images with criterion='nc'
ZOO [30]	58%	6%	89.66%	ImageNet	Inception-v3*	✓	-
DBA [24]	100%	28%	72%	ImageNet	VGG19 [‡]	✓	-
NES-PGD [37]	100%	53%	47%	ImageNet	Inception-v3*	✓	-
Bandits [50]	94%	11%	88.3%	ImageNet	Inception-v3*	✓	-
GenAttack [51]	100%	91%	9%	ImageNet	Inception-v3*	✓	-
DLV [87]	90%	90%	0%	MNIST	NoName*	✓	20 images
Planet [88]	100%	46%	54%	MNIST	testNetworkB.rlv*	✓	Use 'GIVE' model obtain 20 images
MIPVerify [89]	42%	0%	100%	MNIST	MNIST.n1*	✓	Quickstart demo with 100 images
DeepPoly [44]	45%	44%	2.22%	MNIST	convBigRELU_DiffAI*	✓	Gap between $\epsilon = 0.3$ and $\epsilon = 76/255$
DeepGo [90]	25.4%	25.2%	0.78%	MNIST	NoName*	✓	Crafted 1000 images from 1 image
SafeCV [36]	100%	100%	0%	MNIST	NoName*	✓	100 images

Note: * means the target model in the corresponding tool; ‡ means that their tools do not have any target models and we choose widely used target models from Tensorflow or Keras; and *Default* means default input parameters.

used images are shown in the last column in Table III, which depends on the efficiency of the tool under test.

Metrics. We introduce three metrics to evaluate the impacts of the discretization problem. Let N denote the number of input images under test, N_v denote the number of successfully crafted real adversarial examples, and N_i denote the number of integer adversarial examples after the denormalization post-processing,

- Success Rate (SR) is calculated as $\frac{N_v}{N}$,
- True Success Rate (TSR) is calculated as $\frac{N_i}{N}$,
- GAP between SR and TSR is calculated as $\frac{SR-TSR}{SR}$.

To compute N_i , we use the denormalizer provided by the corresponding tools.

1) **RQ1:** To answer this research question, we conduct experiments using default input parameters in their raw papers or tools, which have been widely used by existing works. The results are shown in Table III.

We can observe that 14 out of 20 tools are affected by the discretization problem. Their gaps range from 0.03% to 100%. In more detail, 8 tools have gaps exceeding 50% including white-box testing tools (C&W-L₂, DeepFool, DeepXplore), black-box testing tools (ZOO, DBA and Bandits) and verification tools (Planet and MIPVerify). Among them, 6 tools have gaps exceeding 70%. This demonstrates that if attackers do not pay attention on the discretization problem, they will be likely to generate real adversarial examples which will be damaged after transforming them back into the discrete domain.

There are only 6 out of 20 tools that do not have any gaps including BIM, MBIM, JSMA, DeepConcolic, DLV and SafeCV. These results are largely consistent with our theoretical study.

Answering RQ1: The results on 20 tools show that most of them are affected by the discretization problem. There are 8 tools whose gap exceeds 50%, and 6 tools whose gap exceeds 70%, and only 6 tools do not have any gaps.

2) **RQ2:** To answer this research question, we propose different strategies to tune input parameters for these 14 tools whose gap is not 0 in RQ1. According to our findings in theoretical study, we distinguish these tools by whether the discretization problem can be easily and directly avoided by tuning input parameters.

In theoretical study, the discretization problem can be easily and directly avoided by tuning input parameters. Based on the results in Table III, we can observe that only FGSM has non-zero gap and its discretization problem can be easily and directly avoided by tuning input parameters. The default perturbation step size ϵ used in Table III is 0.3. Therefore, we revise ϵ to $76/255$ in order to avoid the discretization problem. Then, the gap is decreased to 0 with TSR 98.55%. This confirms our theoretical findings.

To illustrate the importance of controllable perturbation step sizes, we also test the implementations of BIM and MBIM in other toolkits, such as Foolbox [97]. Different from the raw implementation of these tools, Foolbox provides a binary search by default. The binary search is performed between the original clean input and the crafted adversarial image, intending to find adversarial boundary. It has been adopted in recent attacks, e.g., [98], [99]. However, if the binary search is implemented without taking into the discretization problem account such as BIM and MBIM in Foolbox, the perturbation step size will become uncontrollable. We use the same input parameters of BIM and MBIM as in RQ1, exception that the binary search is enabled (default in Foolbox). Compared to the results in Table III, the gaps of both BIM and MBIM increase from 0% to 90%. This shows that attackers should pay more

attention on input parameters even the discretization problem is avoidable.

In theoretical study, the discretization problem cannot be easily and directly avoided by tuning input parameters. Based on the results in Table III, there remain 13 tools whose gaps are non-zero, and the discretization problem cannot be easily and directly avoided by tuning input parameters. We do our best to fine-tune input parameters of those tools aimed at increasing TSR and decreasing gap.

First of all, as discussed in theoretical study, the verification tools (i.e., Planet, MIPVerify, DeepPoly and DeepGo) do not provide any parameters to constrain real adversarial examples so that the discretization error could be minimized, we cannot tune input parameters of those tools. For the other 9 test-based tools (i.e., white-box attacks L-BFGS, C&W, DeepFool and DeepXplore, and black-box attacks ZOO, DBA, NES-PGD, Bandits and GenAttack), we adopt the following three strategies to alleviate the discretization problem:

- S1: forbidding adaptive perturbation step size: aims at controlling perturbation step sizes. NES-PGD, DBA, Bandits and GenAttack provide such adaptive mechanism.
- S2: increasing overall perturbations: aims at minimizing the ratio of discretization error against the overall perturbations. L-BFGS, DeepFool, DeepXplore and DBA provide input parameters related to this strategy.
- S3: enhancing strength/confidence of adversarial examples: aims at enhancing the robustness of real adversarial sample. C&W and ZOO provide input parameter related to confidence.

After tuning input parameters, none of them is able to eliminate the discretization errors absolutely.

In terms of TSR, we found that:

- By applying S1, the TSR of NES-PGD and DBA can increase, but the TSR of Bandits and GenAttack cannot;
- By applying S2, the TSR of DBA can increase, but the TSR of DeepXplore, L-BFGS and DeepFool cannot;
- By applying S3, the TSR of C&W- L_2 can increase, but the TSR of ZOO cannot.

This demonstrates that our strategies are able to increase TSR for 3 tools, but fail to increase TSR for the other 6 tools. However, these strategies also bring some side effects, namely, increasing either overall perturbations in terms of Mean Square Error (MSE) or the number of query times, hence sacrificing attack efficiency and imperceptibility of adversarial samples. Due to limited space, detailed statistic is given in Appendix B.

Answering RQ2: According to our experiences, among 14 tools that are affected by the discretization problem, only 1 tool, FGSM, can definitely avoid the discretization problem by tuning input parameters, and only 3 tools can alleviate the discretization problem by tuning input parameters at the cost of attack efficiency or imperceptibility.

Discussion. Our empirical study reveals that the discretization problem is more severe than originally thought in practice,

in conformance with the results of our theoretical study. According to our experimental results, the attack results in published works may not be as good as those reported in raw papers. For instance, DeepFool assumed that the classifier f_t in continuous domain is the same as the classifier in the concrete domain g_t which contradicts to our empirical result, e.g. it has gap 77% in Table III. We believe it is important to highlight the potential impacts of the discretization problem, and by no means invalidate existing methods or their importance and contributions.

It is worth to note that Carlini and Wagner [18] proposed a greedy search based algorithm to alleviate the discretization problem. We conduct an experiment on the greedy search based version of C&W- L_2 which are obtained from Carlini. In our experiment, we use input parameters recommended by Carlini for MNIST images. We found that the greedy search based algorithm significantly improves TSR and reduces gaps without increasing distortions of crafted adversarial examples. This demonstrates that the greedy search based algorithm is a solution to alleviate the discretization problem when one cannot precisely control perturbation step sizes by adjusting input parameters. However, due to the fact that the greedy search based algorithm leverages gradients of targeted networks frequently, it is difficult to integrate it into black-box attacks.

According to our findings, we suggest that: (1) attack success rate should be measured using integer adversarial examples instead of real adversarial examples; (2) it is vital to pay more attention to perturbation step sizes that can be controlled by input parameters; and (3) it is better to revise the implementations of the tools that cannot easily avoid the discretization problem by tuning input parameters if one wants to achieve higher TSR but do not sacrifice the attack efficiency and imperceptibility of adversarial samples.

V. AN APPROACH FOR BLACK-BOX ATTACK

According to our study in Section IV, there lacks an effective and efficient *integer* adversarial example attack in black-box scenario. As a first step towards addressing this problem, we propose a novel black-box algorithm for both targeted and untargeted attacks by presenting a *classification model-based* Derivative-Free discrete Optimization (DFO) method. This type of DFO methods has been widely used to solve complex optimization tasks in a sampling-feedback-style. It does not rely on the gradient of the objective function, but instead, learns from samples of the search space. Therefore, it is suitable for optimizing functions that are non-differentiable, or even unknown but only testable. Furthermore, it was shown by Yu et al. [100] that it is not only superior to many state-of-the-art DFO methods (e.g., genetic algorithm, Bayesian optimization and cross-entropy method), but also stable. We refer readers to [100] for the advantages of classification model-based DFO methods.

In the rest of this section, we first introduce our approach framework, then present the formulation and our algorithm.

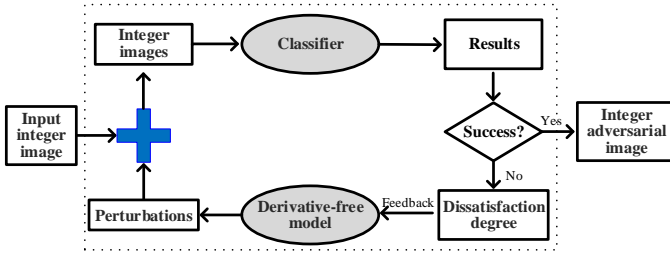


Fig. 2. Framework of our approach DFA.

Threat model. In our black-box scenario, we assume that the adversary knows the input format of the target classifier and has access to the top-k classes and their probabilities for each input image, but he/she does not have any access to any details (e.g., normalization, architecture, parameters and training data) of the target classifier. The distortion of adversarial examples is measured by the \mathbb{L}_∞ distance metric.

A. Framework of DFA

Figure 2 shows the framework of our approach named DFA, standing for **Derivative-Free Attack**. Given an integer image, DFA directly searches an adversarial image in a (discrete integer) search space specified by the maximum \mathbb{L}_∞ distance.

In principle, DFA first samples some perturbations from the search space and then repeats the following procedure until an integer adversarial example is found. During each iteration, DFA queries the target classifier to measure the images (perturbations added onto the input image) via a given *dissatisfaction degree function* which predicates how far is an image from a success attack. The perturbations is partitioned into two parts w.r.t. *dissatisfaction degrees*: perturbations yielding *high* dissatisfaction degrees and perturbations yielding *low* dissatisfaction degrees. The search space is refined into a *small sub-space* according to the partitions of perturbations. New perturbations are sampled from the refined sub-space. Together with old perturbations, a set of best-so-far perturbations is selected according to their dissatisfaction degrees. Finally, the procedure is repeated on the best-so-far perturbations which will be used to refine the sub-space again.

B. Formulation

We formalize the integer adversarial example searching problem as a derivative-free discrete optimization problem by defining the dissatisfaction degree functions. We first introduce some notations.

Let us fix a classifier $f_t : \mathbb{D} \rightarrow \mathbb{C}_t$ for some image classification task t and an integer number ϵ denoting the maximum \mathbb{L}_∞ distance. We denote by $\mathcal{P}(\vec{d})$ the vector of probabilities on the image \vec{d} and by $\mathcal{P}(\vec{d}, c)$ the probability that the image \vec{d} is classified to the class $c \in \mathbb{C}_t$. For a given integer j such that $1 \leq j \leq |\mathbb{C}_t|$, we denote by $\text{Top}_j(\vec{d})$ the j -th largest probability in $\mathcal{P}(\vec{d})$ and $\text{Top}_j^\ell(\vec{d})$ the class whose probability is $\text{Top}_j(\vec{d})$. Obviously, $\text{Top}_1^\ell(\vec{d}) = f_t(\vec{d})$.

We define the initial search space Δ of perturbations as a discrete integer domain $\mathbb{N}_{[-\epsilon, \epsilon]}^{w \times h \times ch}$. Specifically, the discrete domain Δ is a two-dimensional array such that for each

coordinate $p \in P = w \times h \times ch$, $\Delta[p][\text{low}]$ and $\Delta[p][\text{high}]$ (such that $\Delta[p][\text{high}] \geq \Delta[p][\text{low}]$) are integer numbers respectively denoting the lower and upper bound of the value at the coordinate p . Therefore, Δ denotes a set of perturbations such that $\delta \in \Delta$ if and only if $\Delta[p][\text{low}] \leq \delta[p] \leq \Delta[p][\text{high}]$ for all coordinates $p \in P$. The search space Δ will be refined into small sub-spaces by increasing lower bound $\Delta[p][\text{low}]$ or decreasing upper bound $\Delta[p][\text{high}]$ for choosing coordinates p in our algorithm.

Given a perturbation $\delta \in \Delta$, we denote by $\vec{d} \oplus \delta$, the valid image after adding the perturbation δ onto the image \vec{d} , namely, for every coordinate $p \in P$:

$$(\vec{d} \oplus \delta)[p] := \begin{cases} \vec{d}[p] + \delta[p], & \text{if } 0 \leq \vec{d}[p] + \delta[p] \leq 255; \\ 0, & \text{if } \vec{d}[p] + \delta[p] < 0; \\ 255, & \text{if } \vec{d}[p] + \delta[p] > 255. \end{cases}$$

The *integer adversarial example searching problem* with respect to the maximum \mathbb{L}_∞ distance ϵ is to find some perturbation $\delta \in \Delta$ such that:

- $\text{Top}_1^\ell(\vec{d} \oplus \delta) \neq f_t(\vec{d})$ for untargeted attack;
- $\text{Top}_1^\ell(\vec{d} \oplus \delta) = c$ for targeted attack with a target class c .

We solve the integer adversarial example searching problem by reduction to a derivative-free discrete optimization problem. The reduction is given by defining an optimization goal which is characterized by *dissatisfaction-degree functions*. We first consider the untargeted case.

The goal of untargeted attack is to find some perturbation $\delta \in \Delta$ such that $\text{Top}_1^\ell(\vec{d} \oplus \delta) \neq f_t(\vec{d})$. To do this, we maximize the current probability of the image $\vec{d} \oplus \delta$ being classified as the class $\text{Top}_2^\ell(\vec{d} \oplus \delta)$ (i.e., the current class with second largest probability, which may change w.r.t. different δ) until the image is able to successfully mislead the classifier. Therefore, we define the *dissatisfaction-degree function* for untargeted attack, denoted by $D_{\text{ua}}(\cdot, \cdot)$, as follows:

- $D_{\text{ua}}(\vec{d}, \delta) := 0$, if $\text{Top}_1^\ell(\vec{d} \oplus \delta) \neq f_t(\vec{d})$;
- $D_{\text{ua}}(\vec{d}, \delta) := 1 - \text{Top}_2(\vec{d} \oplus \delta)$, otherwise.

In this function, if the attack has succeeded, the perturbation δ is “satisfying”, then the value of the dissatisfaction-degree becomes 0. Otherwise, we return the distance between 1 and the currently reported second largest probability, which is in the range of $[0, 1]$, indicating how far it is from 1. Clearly, in this case, the distance is definitely positive. To this end, our goal is to find a perturbation δ such that the dissatisfaction-degree is 0.

For targeted attack with the target class c , instead of maximizing the probability of $\vec{d} \oplus \delta$ being classified as the class $\text{Top}_2^\ell(\vec{d} \oplus \delta)$, we maximize the probability of the image $\vec{d} \oplus \delta$ being classified as c . Hence, the *dissatisfaction-degree function*, denoted by $D_{\text{ta}}(\cdot, \cdot)$, is defined as follows:

- $D_{\text{ta}}(\vec{d}, \delta) := 0$, if $\text{Top}_1^\ell(\vec{d} \oplus \delta) = c$;
- $D_{\text{ta}}(\vec{d}, \delta) := 1 - \mathcal{P}((\vec{d} \oplus \delta), c)$, otherwise.

Now, the integer adversarial example searching problem is reduced to the minimization problem of the dissatisfaction-degree functions.

C. Algorithm

Instead of using heuristic search methods, e.g. genetic programming, particle swarm optimization, simulated annealing, to solve the minimization problem of the dissatisfaction-degree functions, we propose a classification model-based DFO method (shown in Algorithm 1). Different from heuristic search based methods, our method maintains a classification model during the search to distinguish “good” samples from “bad” samples. Then, the search space Δ will be refined by learning from the samples to help to converge to the best solution.

In detail, Algorithm 1 first initializes the search space Δ according to the given maximum \mathbb{L}_∞ distance ϵ (Line 1). Then, it randomly selects $(s + k)$ perturbations (stored as the set B_0) from the search space Δ (Line 2), where s denotes the sample size during each iteration and k denotes the ranking threshold. Next, it computes $(s + k)$ valid images by adding the perturbations onto the source integer image \vec{d} (Line 3) and evaluates the dissatisfaction-degree (d.d.) of these images using the dissatisfaction-degree function D (Line 4). The perturbation \tilde{x} with the smallest dissatisfaction-degree is selected from the set B_0 (Line 5). After that, Algorithm 1 repeats the following procedure.

For each iteration $t \geq 1$, if the perturbation \tilde{x} suffices to craft an integer adversarial example, return \tilde{x} (Lines 7-8). Otherwise, the set B_{t-1} of perturbations is partitioned into two sets: “positive” set B_{t-1}^+ and “negative” set B_{t-1}^- , where B_{t-1}^+ consists of the smallest- k perturbations in terms of the dissatisfaction-degree (Lines 9-10).

Based on B_{t-1}^+ and B_{t-1}^- , Algorithm 1 refines the search space Δ into a small sub-space (Lines 11-35) as follows. It first randomly selects a sample b^+ from the positive set B_{t-1}^+ (Line 13) and randomly selects u coordinates to refine (Lines 15-27). For each selected coordinate p , it compares the number of perturbations in B_{t-1}^- whose value is larger than the value of b^+ at the coordinate p against the number of perturbations in B_{t-1}^+ whose value is smaller than the value of b^+ at the coordinate p . If the majority of perturbations in B_{t-1}^- are larger than b^+ at the coordinate p , we decrease the upper bound of the search space Δ (Lines 21-23), otherwise increase the lower bound (Lines 25-27), at the coordinate p . Once u coordinates have been processed, we craft a new image b' from b^+ by reassigning the value of each coordinate $p \in Y$ with the random integer r from $\Delta[p][\text{low}]$ to $\Delta[p][\text{high}]$ (Lines 29-33). The new perturbation b' is added into the set B . Then, the search space Δ is reset to the original size. We remark that the refining procedure for the next sample will be conducted on the original search space to avoid over fitting.

When the search space Δ has been refined s times, we get s new perturbations (i.e., set B), resulting in $(2s + k)$ perturbations in the set $B \cup B_{t-1}$. From them, we choose the smallest- $(s + k)$ perturbations in terms of the dissatisfaction-degree (Line 37). Algorithm 1 continues the above procedure on B_t until an integer adversarial example is found or the number of iterations T is reached.

Algorithm 1: A DFO-based algorithm

Input: classifier under attack $f_t : \mathbb{D} \rightarrow \mathbb{C}_t$, integer image $\vec{d} \in \mathbb{D}$, number of iterations $T \in \mathbb{N}$, ranking threshold $k \in \mathbb{N}$, sample size $s \in \mathbb{N}$, maximum \mathbb{L}_∞ distance $\epsilon \in \mathbb{N}$, the number of coordinates to be changed in each refinement process $u \in \mathbb{N}$, dissatisfaction-degree (d.d.) function D

Output: optimized perturbation \tilde{x}

```

1:  $\Delta = \mathbb{N}_{[-\epsilon, \epsilon]}^{w \times h \times ch}$ ;
2:  $B_0 = \{\delta_1, \dots, \delta_{s+k}\}$  sampled from  $\Delta$ ; // initial collection
3: Evaluate the dissatisfaction-degree  $D(\vec{d}, \delta_i)$  for  $1 \leq i \leq s + k$ ;
4:  $\tilde{x} = \operatorname{argmin}_{\delta \in B_0} D(\vec{d}, \delta)$ ; // select the best-so-far sample
5: for  $t = 1$  to  $T$  do
6:   if  $D(\vec{d}, \tilde{x}) = 0$  then
7:     break; // find an adversarial example
8:    $B_{t-1}^+ =$  smallest- $k$  solutions in  $B_{t-1}$  in terms of d.d.;
9:    $B_{t-1}^- = B_{t-1} - B_{t-1}^+$ ;
10:   $B = \emptyset$ ;
11:  for  $i = 1$  to  $s$  do
12:    // Refine the space  $\Delta$  into a small one by  $B_{t-1}^+$  and  $B_{t-1}^-$ 
13:    Randomly select a sample  $b^+$  from the positive set  $B_{t-1}^+$ ;
14:     $Y = \emptyset$ ;
15:    for  $j = 1$  to  $u$  do
16:      Randomly select a coordinate  $p$  from  $P = w \times h \times ch$ ;
17:       $Y = Y \cup \{p\}$ ;
18:       $\mathbf{ge} := \{b \in B_{t-1}^- \mid b[p] > b^+[p]\}$ ;
19:       $\mathbf{le} := \{b \in B_{t-1}^+ \mid b[p] < b^+[p]\}$ ;
20:      if  $|\mathbf{ge}| > |\mathbf{le}|$  then
21:         $\mathbf{minVal} = \min_{b \in \mathbf{ge}} b[p]$ ;
22:        Randomly select an integer  $r$  from  $\mathbf{minVal}$  to  $b^+[p]$ ;
23:         $\Delta[p][\mathbf{high}] = r$ ; // decrease the upper bound at  $p$ 
24:      else
25:         $\mathbf{maxVal} = \max_{b \in \mathbf{le}} b[p]$ ;
26:        Randomly select an integer  $r$  from  $b^+[p]$  to  $\mathbf{maxVal}$ ;
27:         $\Delta[p][\mathbf{low}] = r$ ; // increase the lower bound at  $p$ 
28:       $b' = \text{Copy of } b^+$ ;
29:      for  $p \in Y$  do
30:        // Sample in the refined the search space  $\Delta$ 
31:        Randomly select an integer  $r$  from  $\Delta[p][\mathbf{low}]$  to
32:           $\Delta[p][\mathbf{high}]$ ;
33:         $b'[p] = r$ ;
34:         $B = B \cup \{b'\}$ ;
35:         $\Delta = \mathbb{N}_{[-\epsilon, \epsilon]}^{w \times h \times ch}$ ;
36:        // Reset Delta for next sample to avoid over fitting
37:      Evaluate the dissatisfaction-degree  $D(\vec{d}, \delta)$  for all  $\delta \in B$ ;
38:       $B_t =$  smallest- $(s + k)$  solutions in  $B \cup B_{t-1}$  in terms of
39:        dissatisfaction-degree // keep the size as  $s + k$ ;
40:       $\tilde{x} = \operatorname{argmin}_{\delta \in B_t} D(\vec{d}, \delta)$ ;
41:    return  $\tilde{x}$ ;

```

Dimensionality reduction. Algorithm 1 depicts the main workflow of our approach which solves the integer adversarial example searching problem by a classification model-based DFO method. It can be further optimized by a dimensionality reduction technique, which reduces the search space Δ into a lower dimensional space, to improve query efficiency. Dimensionality reduction has been adopted in recent attacks, e.g., AutoZOOM [34] and GenAttack [51]. Instead of searching in the large search space $\Delta = \mathbb{N}_{[-\epsilon, \epsilon]}^{w \times h \times ch}$, we can first search a perturbation δ_r in a small search space $\Delta_r = \mathbb{N}_{[-\epsilon, \epsilon]}^{w_r \times h_r \times ch}$ for $w_r \leq w$ and $h_r \leq h$, and scale δ_r up to δ_o with the same size as input (i.e. the search space Δ) by applying resizing methods

(e.g., bilinear resizing), resulting in the valid image $\vec{d} \oplus \delta_o$ in the original size. (Please refer to [34] and [51] for the more details of dimensionality reduction.) By doing so, the query efficiency of our method can be improved while maintaining the attack success rate under the \mathbb{L}_∞ constraint.

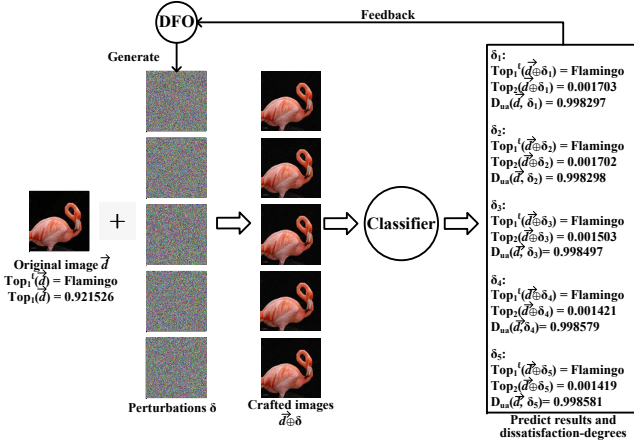


Fig. 3. Untargeted attack on a Flamingo image (the first iteration).

D. Illustrative Example

We illustrate Algorithm 1 through an example, as shown in Figure 3. The original integer image \vec{d} is an image from the ImageNet dataset and it is classified as the class *flamingo* by the target classifier Inception-v3. To launch untargeted attack using this image, we set the sample size s as 3 and the ranking threshold k as 2. Consider the first iteration, Algorithm 1 samples 5 perturbations $(\delta_i)_{1 \leq i \leq 5}$ from $\Delta = \mathbb{N}_{[-20, 20]}^{w \times h \times ch}$ and adds them onto the original image, resulting in five new images (shown in Figure 3). Then, it computes the dissatisfaction degrees of these five new images $(\vec{d} \oplus \delta_i)_{1 \leq i \leq 5}$ by querying the classifier and the dissatisfaction-degree function D_{ua} . Among these 5 perturbations, $(\vec{d} \oplus \delta_1)$ has the smallest dissatisfaction degree, hence δ_1 is the best-so-far perturbation. After more iterations, the results are shown in Figure 4. We can see that after the 388-th iteration, the image with smallest dissatisfaction degree is classified as the class *hook*, but is visually indistinguishable from the original one.

E. Scenario Extension

Our framework is very reflexible and could be potentially adapted to other scenarios such as: (1) target classifiers that only output *top-1 class* and *its probability*, and (2) target classifiers that are integrated with defenses, by restricting the search space or modifying dissatisfaction-degree functions.

For instance, if the adversary only have access to the top-1 class and its probability, the dissatisfaction-degree function for untargeted attack can be adapted as follows:

- $D_{ua}^1(\vec{d}, \delta) := 0$, if $\text{Top}_1^l(\vec{d} \oplus \delta) \neq f_t(\vec{d})$;
- $D_{ua}^1(\vec{d}, \delta) := \text{Top}_1(\vec{d} \oplus \delta)$, otherwise.

The dissatisfaction-degree function for targeted attack could be adapted accordingly. Remark that it is different from label-only attacks in which the adversary has access to the top-1 class, but *not* its probability. We leave this to future work.

TABLE IV
EXPERIMENT SETTINGS

Parameter	Setting
Max. \mathbb{L}_∞ distance ϵ	$\epsilon = 64$ for MNIST and $\epsilon = 10$ for ImageNet.
Target class	For MNIST images, the class with 4-th largest probability is chosen as the target class. For ImageNet images, the class with 11-th largest probability is chosen as the target class.
Sample size s	$s = 3$ in all the experiments.
Ranking Threshold k	$k = 2$ in all the experiments.
Coordinate	$u = 2$ pixels for MNIST images.
Threshold u	$u = 10$ pixels for ImageNet images.
Iteration Threshold T	$T = 30000$ in all the experiments.
Timeout Threshold	3 minutes for MNIST images. 30 minutes for ImageNet images.
Resized Space Δ_r	No resize for MNIST images. $100 \times 100 \times 3$ for ImageNet images.

VI. IMPLEMENTATION AND EVALUATION

We implement our classification model-based DFO method in DFA based on the framework of RACOS [100], for which we implement our new algorithm and manage to engineer to significantly improve its efficiency and scalability with lots of domain-specific optimizations. Hereafter, we report experimental results compared with state-of-the-art white-box and black-box attacks.

A. Dataset & Setting

Dataset. We use two standard datasets MNIST [46] and ImageNet [48]. MNIST is a dataset of handwritten digits with 10 classes (0-9). We choose the first 200 images out of 10000 validation images of MNIST as our subjects.

We use the same 100 ImageNet images as in Section IV-C. (Recall that we randomly choose 100 classes from which we randomly choose 1 image per class that can be correctly classified by four classifiers in Keras: ResNet50, Inception-v3, VGG16 and VGG19.)

Target model. For MNIST images, we use a DNN classifier LeNet-1 from the LeNet family [47]. LeNet-1 is a popular target model for MNIST images, e.g., [22], [38], [101]–[103]. For ImageNet images, we use a pre-trained DNN classifier Inception-v3 [49] which is a widely used target model for ImageNet images, e.g., [18], [30], [34], [37], [51].

Setting. As shown in Section IV-C, the discretization problem can be avoided or alleviated by tuning input parameters for some tools, at the cost of attack efficiency or quality of adversarial examples, except for FGSM and C&W+GS. Therefore, to maximize their TSRs as done in Section IV-C, we choose proper step sizes for FGSM and enable greedy search for C&W+GS with parameters recommended by Carlini on MNIST images. For other tools, we use the parameters as in their raw papers which are already fine-tuned by the authors.

We conduct both untargeted attack and targeted attack on a Linux PC running UBUNTU 16.04 LTS with Intel Xeon(R) W-2123 CPU, TITAN Xp COLLECTORS GPU and 64G RAM. Table IV lists the other experiment settings.

B. Comparison with White-Box Methods

Although our method is a black-box one, we compare the performance with four well-known white-box tools: FGSM,

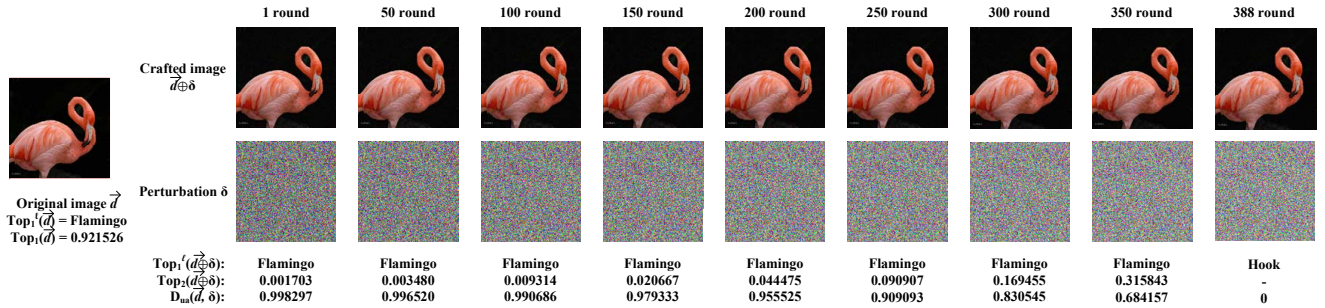


Fig. 4. Illustrative example of an untargeted attack on a *Flamingo* image.

TABLE V
RESULTS OF WHITE-BOX UNTARGETED ATTACKS

Dataset & DNN	Method	SR	TSR	GAP
MNIST LeNet-1	FGSM	97%	97%	0%
	BIM	100%	100%	0%
	C&W	100%	88%	12%
	C&W+GS	100%	100%	0%
	DFA	100%	100%	0%
ImageNet Inception-v3	FGSM	79%	79%	0%
	BIM	100%	100%	0%
	C&W	100%	68%	32%
	DFA	99%	99%	0%

Note: C&W+GS only implements attacks for MNIST images.

TABLE VI
RESULTS OF WHITE-BOX TARGETED ATTACKS

Dataset & DNN	Method	SR	TSR	GAP
MNIST LeNet-1	FGSM-1	84%	84%	0%
	BIM	100%	100%	0%
	C&W	100%	75%	25%
	C&W+GS	100%	100%	0%
	DFA	100%	100%	0%
ImageNet Inception-v3	FGSM-1	9%	9%	0%
	BIM	99%	99%	0%
	C&W	100%	24%	76%
	DFA	96%	96%	0%

BIM, C&W and C&W+GS, where the implementations are by their authors. Since FGSM has nearly no ability to handle targeted attack, we use one-step target class method (denoted by FGSM-1) of [104], which can be regarded as the targeted version of FGSM. The maximum \mathbb{L}_∞ distances are transformed into their maximum \mathbb{L}_2 distances accordingly.

The results are shown in Table V and Table VI for untargeted and targeted attacks, respectively. Overall, our attack DFA achieves close to 100% attack success rates for both targeted and untargeted attacks. In terms of SR, our tool DFA outperforms FGSM/FGSM-1 and is comparable to the other tools. In terms of TSR, DFA is comparable to BIM and outperforms FGSM, FGSM-1 and C&W in most cases.

Specifically, FGSM, FGSM-1, BIM and C&W+GS do not have any gap due to the tuning of step sizes and the greedy search based algorithm. It is easy to observe that C&W has a relatively larger gap in targeted attacks on Inception-v3 in \mathbb{L}_∞ norm setting, as its TSR is only 24% compared with 100% SR. Thus, although C&W outperforms DFA in terms of SR, DFA outperforms C&W in most cases in terms of TSR. We remark that the gap of C&W is slightly different from the one given in Table III, as C&W- \mathbb{L}_2 has an input parameter κ which can

control the confidence. By increasing κ , the confidence of real adversarial examples as well as the TSR of C&W- \mathbb{L}_2 increase, and the gap can be minimized. Whereas C&W- \mathbb{L}_∞ does not have this parameter.

C. Comparison with Black-Box Methods

We compare DFA with well-known recent black-box methods: substitute model based attacks, ZOO, NES-PGD, FD, FD-PSO, and also three concurrent works Bandits, AutoZOOM and GenAttack, representing all the classes of existing black-box attacks (cf. Section II), where the implementations are by their authors.

Recall that it is very difficult to tune input parameters for those tools without loss of attack efficiency or quality of adversarial examples, hence we use the parameters as in their raw papers which are already fine-tuned by the authors. When evaluating substitute model, we use FGSM/FGSM-1 and C&W methods, and use ResNet50 [105] as the substitute model for Inception-v3, the model in ZOO as the substitute model for LeNet-1. Since ZOO and AutoZOOM use \mathbb{L}_2 distance, we map our maximum \mathbb{L}_∞ distances into maximum \mathbb{L}_2 distances by considering the worst case of \mathbb{L}_∞ , namely, all the pixels are modified by the maximum \mathbb{L}_∞ distance. For instance, the \mathbb{L}_∞ distance 10 is approximated by \mathbb{L}_2 distance $\sqrt{(10/255)^2 \times (299 \times 299 \times 3)} \approx 20$ for $299 \times 299 \times 3$ images. Remark that this is not a rigorous mapping, ZOO and AutoZOOM under \mathbb{L}_2 would be easier to find an adversarial example, as the corresponding \mathbb{L}_2 distances are less restricted.

The results of untargeted and targeted attacks are given in Table VII and Table VIII. We can see that our attack DFA achieves close to 100% attack success rates for both targeted and untargeted attacks and outperforms all the other tools in terms of TSR no matter targeted or untargeted attacks. In terms of SR, our tool is also comparable (or better) to the other tools.

D. Query Comparison.

In many black-box scenarios, the attacker has a limited number of queries to the classifier. Therefore, we report the average number of queries of the black-box attacks in Table IX, where substitute model based attack is excluded due to its low SR. We remark that ZOO is regarded as baseline, the others are state-of-the-art query-efficient tools.

TABLE VII
RESULTS OF BLACK-BOX UNTARGETED ATTACKS

Dataset & DNN	Method	SR	TSR	GAP
MNIST LeNet-1	SModel+C&W	2.5%	2.5%	0%
	SModel+FGSM	20%	20%	0%
	FD	94.5%	94.5%	0%
	FD-PSO	46.5%	46.5%	0%
	DFA	100%	100%	0%
ImageNet Inception-v3	SModel+C&W	6%	6%	0%
	SModel+FGSM	38%	38%	0%
	ZOO	89%	5%	94.3%
	AutoZOOM	100%	57%	43%
	NES-PGD	100%	77%	23%
	Bandits	100%	12%	88%
	GenAttack	100%	93%	7%
	DFA	99%	99%	0%

Note: FD and FD-PSO do not provide attacks against ImageNet images. ZOO and AutoZOOM do not provide attacks under L_∞ distance, so we only compare our tool with them on ImageNet images. NES-PGS and Bandits do not provide attacks against MNIST images. Meanwhile, the version of GenAttack’s attack against MNIST is buggy.

TABLE VIII
RESULTS OF BLACK-BOX TARGETED ATTACKS

Dataset & DNN	Method	SR	TSR	GAP
MNIST LeNet-1	SModel+C&W	1.5%	1.5%	0%
	SModel+FGSM-1	5%	5%	0%
	FD	72%	72%	0%
	FD-PSO	6.5%	6.5%	0%
	DFA	100%	100%	0%
ImageNet Inception-v3	SModel+C&W	1%	1%	0%
	SModel+FGSM-1	2%	2%	0%
	ZOO	69%	5%	92.7%
	AutoZOOM	95%	43%	54.7%
	NES-PGD	100%	47%	53%
	GenAttack	100%	84%	16%
DFA	96%	96%	0%	

Note: Bandits does not support targeted attack.

On attack against Inception-v3, our tool DFA outperforms all the other tools for targeted attacks, except for GenAttack, which is slightly better than DFA. For untargeted attacks, our tool DFA outperforms the baseline tool ZOO and comparable to other tools. Recall that our tool DFA outperforms all these tools in terms of TSR.

We remark that ZOO and AutoZOOM are tested under the L_2 distance 20, which is less restricted than the L_∞ distance 10 used for the other tools. Indeed, in untargeted attack setting, the average L_2 distance of our tool is 8.33. Whereas the average query times of AutoZOOM becomes 4971 (worse than ours) if $L_2 = 12$.

On attack against LeNet-1, our tool DFA outperforms both of them in almost all cases, exception that FD uses less query times than DFA for targeted attacks. Note that our tool DFA achieves higher attack success attack rate than FD and FD-PSO in terms of both SR/TSR. One may notice that the query times of FD and FD-PSO are same between untargeted and targeted attacks. This is due to the implementations of FD and FD-PSO (confirmed by some authors of [52]).

Furthermore, we also report the average Mean Square Error (MSE) of the adversarial examples in Table IX. We can observe that our tool DFA outperforms most of the other tools on attacks against Inception-v3. FD and FD-PSO are slightly better than DFA on attacks against LeNet-1, at the same order of magnitude. ZOO outperforms all the other tools in terms

TABLE IX
COMPARISON WITH AVERAGE QUERY TIMES AND CORRESPONDING MSE

Dataset & DNN	Method	Untargeted		Targeted	
		Query	MSE	Query	MSE
MNIST LeNet-1	FD	1568	3.4e-2	1568	3.5e-2
	FD-PSO	10000	2.5e-2	10000	2.5e-2
	DFA	817	3.7e-2	1593	5.1e-2
	ZOO	85368	1.7e-5	203683	3.6e-5
ImageNet Inception-v3	AutoZOOM	2224	9.2e-4	14322	1.2e-3
	NES-PGD	4741	8.4e-4	13421	9.0e-4
	Bandits	4595	1.4e-3	-	-
	GenAttack	4008	6.3e-4	12369	9.2e-4
	DFA	4746	2.6e-4	12740	3.4e-4

Note: The queries of our tool is computed on integer adversarial examples, while it is computed on real adversarial examples for the others.

of MSE against Inception-v3, but at the cost of huge number of query times.

E. Attack Classifiers with Defense

To show the effectiveness of our approach, we use our tool to attack the HGD defense [53], which won the first place of NIPS 2017 competition on defense against adversarial attacks. HGD defense is a typical denoising based defending methods for image classification. The whole classification system is an ensemble of 4 independent models and their denoiser (ResNet, ResNext, InceptionV3, inceptionResNetV2). We conduct untargeted attacks against this model using the same 100 ImageNet images and parameters as previously, exception that the L_∞ distance ϵ is 32 according to the NIPS 2017 competition. Our tool achieves 100% TSR in the experiments, indicating the effectiveness of DFA.

MNIST Adversarial Examples Challenge [54] is another widely recognized attack problem. It uses adversarial training for defending. We use the same 200 MNIST images as previously on the attack of this problem. Our tool DFA achieves 10.5% TSR, the same as the current best white-box attack “interval attacks”, which is publicly reported on the webpage of the challenge. The images on which the attacks succeed by both methods are exactly same, and the time costs of both tools are also similar.

VII. CONCLUSION

We conducted the first comprehensive study of 35 methods and 20 open source tools for crafting adversarial examples, in an attempt to understand the impacts of the discretization problem. Our study revealed that most of these methods and tools are affected by this problem and researchers should pay more attention when designing adversarial example attacks and measuring attack success rate. We also proposed strategies to avoid or alleviate the discretization problem, which can improve TSR of some tools, at the cost of attack efficiency or imperceptibility of adversarial examples.

We proposed a black-box method by designing a classification model-based derivative-free optimization method. Our method directly crafts adversarial examples in discrete integer domains, hence does not have the discretization problem and is able to attack a wide range of classifiers including non-differentiable ones. Our attack method requires access

to the probability distribution of classes for each test input and does not rely on the gradient of the objective function, but instead, learns from samples of the search space. We implemented our method into tool DFA, and conducted an intensive set of experiments on MNIST and ImageNet in both untargeted and targeted scenarios. The experimental results show that our method achieved close to 100% attack success rate, comparable to the white-box methods (FGSM, BIM and C&W) and outperformed the state-of-the-art black-box methods. Moreover, our method achieved 100% success rate on the winner of NIPS 2017 competition on defense, and achieved the same result as the best white-box attack in MNIST Challenge. Our results suggest that classification model-based derivative-free discrete optimization opens up a promising research direction into effective black-box attacks.

REFERENCES

- [1] P. Holley, "Texas becomes the latest state to get a self-driving car service," <https://www.washingtonpost.com/news/innovations/wp/2018/05/07/texas-becomes-the-latest-state-to-get-a-self-driving-car-service>, May 2018.
- [2] Apollo, "An open, reliable and secure software platform for autonomous driving systems," <http://apollo.auto>, 2018.
- [3] Waymo, "A self-driving technology development company," <https://waymo.com/>, 2009.
- [4] D. C. Ciresan, A. Giusti, L. M. Gambardella, and J. Schmidhuber, "Deep neural networks segment neuronal membranes in electron microscopy images," in *Proceedings of the 26th Annual Conference on Neural Information Processing Systems.*, 2012, pp. 2852–2860.
- [5] D. Shen, G. Wu, , and H.-I. Suk, "Deep learning in medical image analysis," *Annual Review of Biomedical Engineering*, vol. 19, pp. 221–248, 2017.
- [6] T. Parag, D. C. Ciresan, and A. Giusti, "Efficient classifier training to minimize false merges in electron microscopy segmentation," in *Proceedings of 2015 IEEE International Conference on Computer Vision*, 2015, pp. 657–665.
- [7] F. Zhang, J. Leitner, M. Milford, B. Upcroft, and P. I. Corke, "Towards vision-based deep reinforcement learning for robotic motion control," *CoRR*, vol. abs/1511.03791, 2015.
- [8] S. Levine, P. Pastor, A. Krizhevsky, J. Ibarz, and D. Quillen, "Learning hand-eye coordination for robotic grasping with deep learning and large-scale data collection," *I. J. Robotics Res.*, vol. 37, no. 4-5, pp. 421–436, 2018.
- [9] E. C. R. Shin, D. Song, and R. Moazzezi, "Recognizing functions in binaries with neural networks," in *Proceedings of the 24th USENIX Security Symposium, USENIX Security*, 2015, pp. 611–626.
- [10] W. Song, H. Yin, C. Liu, and D. Song, "Deepmem: Learning graph neural network models for fast and robust memory forensic analysis," in *Proceedings of the 2018 ACM SIGSAC Conference on Computer and Communications Security*, 2018, pp. 606–618.
- [11] L. D. L. Rosa, S. Kilgallon, T. Vanderbruggen, and J. Cavazos, "Efficient characterization and classification of malware using deep learning," in *2018 Resilience Week (RWS)*, 2018, pp. 77–83.
- [12] N. N. Dalvi, P. M. Domingos, Mausam, S. K. Sanghai, and D. Verma, "Adversarial classification," in *Proceedings of the Tenth ACM SIGKDD International Conference on Knowledge Discovery and Data Mining*, 2004, pp. 99–108.
- [13] C. Szegedy, W. Zaremba, I. Sutskever, J. Bruna, D. Erhan, I. Goodfellow, and R. Fergus, "Intriguing properties of neural networks," in *Proceedings of International Conference on Learning Representations*, 2014.
- [14] B. Li and Y. Vorobeychik, "Feature cross-substitution in adversarial classification," in *Proceedings of Advances in Neural Information Processing Systems*, 2014, pp. 2087–2095.
- [15] I. Goodfellow, J. Shlens, and C. Szegedy, "Explaining and harnessing adversarial examples," in *International Conference on Learning Representations*, 2014.
- [16] A. M. Nguyen, J. Yosinski, and J. Clune, "Deep neural networks are easily fooled: High confidence predictions for unrecognizable images," in *Proceedings of 2015 IEEE Conference on Computer Vision and Pattern Recognition*, 2015, pp. 427–436.
- [17] N. Carlini and D. A. Wagner, "Adversarial examples are not easily detected: Bypassing ten detection methods," in *Proceedings of the 10th ACM Workshop on Artificial Intelligence and Security*, 2017, pp. 3–14.
- [18] —, "Towards evaluating the robustness of neural networks," in *2017 IEEE Symposium on Security and Privacy*, 2017, pp. 39–57.
- [19] N. Papernot, P. D. McDaniel, S. Jha, M. Fredrikson, Z. B. Celik, and A. Swami, "The limitations of deep learning in adversarial settings," in *Proceedings of IEEE European Symposium on Security and Privacy*, 2016, pp. 372–387.
- [20] M. Sharif, S. Bhagavatula, L. Bauer, and M. K. Reiter, "Accessorize to a crime: Real and stealthy attacks on state-of-the-art face recognition," in *Proceedings of the 2016 ACM SIGSAC Conference on Computer and Communications Security*, 2016, pp. 1528–1540.
- [21] S.-M. Moosavi-Dezfooli, A. Fawzi, O. Fawzi, and P. Frossard, "Universal adversarial perturbations," in *Proceedings of 2017 IEEE Conference on Computer Vision and Pattern Recognition*, 2017, pp. 86–94.
- [22] K. Pei, Y. Cao, J. Yang, and S. Jana, "Deepxplore: Automated whitebox testing of deep learning systems," in *Proceedings of the 26th Symposium on Operating Systems Principles*, 2017, pp. 1–18.
- [23] A. Kurakin, I. Goodfellow, and S. Bengio, "Adversarial examples in the physical world," in *Proceedings of International Conference on Learning Representations*, 2017.
- [24] W. Brendel, J. Rauber, and M. Bethge, "Decision-based adversarial attacks: Reliable attacks against black-box machine learning models," in *International Conference on Learning Representations*, 2018.
- [25] C. Xiao, J.-Y. Zhu, B. Li, W. He, M. Liu, and D. Song, "Spatially transformed adversarial examples," in *International Conference on Learning Representations*, 2018.
- [26] Z. Zhao, D. Dua, and S. Singh, "Generating natural adversarial examples," in *International Conference on Learning Representations*, 2018.
- [27] J. Kos, I. Fischer, and D. Song, "Adversarial examples for generative models," in *Proceedings of 2018 IEEE Security and Privacy Workshops*, 2018, pp. 36–42.
- [28] K. Eykholt, I. Evtimov, E. Fernandes, B. Li, A. Rahmati, C. Xiao, A. Prakash, T. Kohno, and D. Song, "Robust physical-world attacks on deep learning visual classification," in *Proceedings of 2018 IEEE Conference on Computer Vision and Pattern Recognition*, 2018, pp. 1625–1634.
- [29] A. Athalye, L. Engstrom, A. Ilyas, and K. Kwok, "Synthesizing robust adversarial examples," in *Proceedings of the 35th International Conference on Machine Learning*, 2018, pp. 284–293.
- [30] P. Chen, H. Zhang, Y. Sharma, J. Yi, and C. Hsieh, "ZOO: zeroth order optimization based black-box attacks to deep neural networks without training substitute models," in *Proceedings of the 10th ACM Workshop on Artificial Intelligence and Security*, 2017, pp. 15–26.
- [31] A. Ilyas, L. Engstrom, A. Athalye, and J. Lin, "Query-efficient black-box adversarial examples," *arXiv preprint arXiv:1712.07113*, 2017.
- [32] N. Papernot, P. D. McDaniel, I. J. Goodfellow, S. Jha, Z. B. Celik, and A. Swami, "Practical black-box attacks against machine learning," in *Proceedings of the 2017 ACM on Asia Conference on Computer and Communications Security*, 2017, pp. 506–519.
- [33] A. N. Bhagoji, W. He, B. Li, and D. Song, "Exploring the space of black-box attacks on deep neural networks," *CoRR*, vol. abs/1712.09491, 2017.
- [34] C. Tu, P. Ting, P. Chen, S. Liu, H. Zhang, J. Yi, C. Hsieh, and S. Cheng, "Autozoom: Autoencoder-based zeroth order optimization method for attacking black-box neural networks," in *The Thirty-Third AAAI Conference on Artificial Intelligence*, 2019, pp. 742–749.
- [35] M. Cheng, T. Le, P. Chen, J. Yi, H. Zhang, and C. Hsieh, "Query-efficient hard-label black-box attack: An optimization-based approach," *CoRR*, vol. abs/1807.04457, 2018.
- [36] M. Wicker, X. Huang, and M. Kwiatkowska, "Feature-guided black-box safety testing of deep neural networks," in *Proceedings of the 24th International Conference on Tools and Algorithms for the Construction and Analysis of Systems*, 2018, pp. 408–426.
- [37] A. Ilyas, L. Engstrom, A. Athalye, and J. Lin, "Black-box adversarial attacks with limited queries and information," in *Proceedings of the 35th International Conference on Machine Learning*, 2018, pp. 2142–2151.
- [38] L. Ma, F. Juefei-Xu, F. Zhang, J. Sun, M. Xue, B. Li, C. Chen, T. Su, L. Li, Y. Liu, J. Zhao, and Y. Wang, "Deepgauge: multi-granularity testing criteria for deep learning systems," in *Proceedings of the 33rd ACM/IEEE International Conference on Automated Software Engineering*, 2018, pp. 120–131.
- [39] G. Katz, C. W. Barrett, D. L. Dill, K. Julian, and M. J. Kochenderfer, "Reluplex: An efficient SMT solver for verifying deep neural networks," in *Proceedings of the 29th International Conference on Computer Aided Verification*, 2017, pp. 97–117.
- [40] L. Pulina and A. Tacchella, "An abstraction-refinement approach to verification of artificial neural networks," in *Proceedings of the 22nd International Conference on Computer Aided Verification (CAV)*, 2010, pp. 243–257.
- [41] T. Gehr, M. Mirman, D. Drachler-Cohen, P. Tsankov, S. Chaudhuri, and M. T. Vechev, "AI2: safety and robustness certification of neural networks with abstract interpretation," in *Proceedings of the 2018 IEEE Symposium on Security and Privacy*, 2018, pp. 3–18.
- [42] D. Gopinath, G. Katz, C. S. Pasareanu, and C. Barrett, "DeepSAFE: A data-driven approach for assessing robustness of neural networks," in *Proceedings of the 16th International Symposium on Automated Technology for Verification and Analysis*, 2018, pp. 3–19.
- [43] G. Singh, T. Gehr, M. Mirman, M. Püschel, and M. T. Vechev, "Fast and effective robustness certification," in *Advances in Neural Information Processing Systems*, 2018, pp. 10825–10836.

- [44] G. Singh, T. Gehr, M. Püschel, and M. Vechev, "An abstract domain for certifying neural networks," in *POPL*, 2019.
- [45] I. J. Goodfellow, Y. Bengio, and A. C. Courville, *Deep Learning*, ser. Adaptive computation and machine learning. MIT Press, 2016.
- [46] Y. LeCun, C. Cortes, and C. J. Burges, "The mnist database of handwritten digits," 1998.
- [47] Y. Lecun, L. Bottou, Y. Bengio, and P. Haffner, "Gradient-based learning applied to document recognition," *Proceedings of the IEEE*, vol. 86, no. 11, pp. 2278–2324, 1998.
- [48] J. Deng, W. Dong, R. Socher, L. Li, K. Li, and F. Li, "Imagenet: A large-scale hierarchical image database," in *2009 IEEE Computer Society Conference on Computer Vision and Pattern Recognition (CVPR)*, 2009, pp. 248–255.
- [49] C. Szegedy, V. Vanhoucke, S. Ioffe, J. Shlens, and Z. Wojna, "Rethinking the inception architecture for computer vision," in *2016 IEEE Conference on Computer Vision and Pattern Recognition (CVPR)*, 2016, pp. 2818–2826.
- [50] A. Ilyas, L. Engstrom, and A. Madry, "Prior convictions: Black-box adversarial attacks with bandits and priors," in *7th International Conference on Learning Representations (ICLR)*, 2019.
- [51] M. Alzantot, Y. Sharma, S. Chakraborty, H. Zhang, C. Hsieh, and M. B. Srivastava, "Genattack: practical black-box attacks with gradient-free optimization," in *Proceedings of the Genetic and Evolutionary Computation Conference*, 2019, pp. 1111–1119.
- [52] A. N. Bhagoji, W. He, B. Li, and D. Song, "Practical black-box attacks on deep neural networks using efficient query mechanisms," in *Proceedings of the 15th European Conference on Computer Vision (ECCV)*, 2018, pp. 158–174.
- [53] F. Liao, M. Liang, Y. Dong, T. Pang, X. Hu, and J. Zhu, "Defense against adversarial attacks using high-level representation guided denoiser," in *2018 IEEE Conference on Computer Vision and Pattern Recognition, CVPR*, 2018, pp. 1778–1787.
- [54] M. Lab, "MNIST adversarial examples challenge," https://github.com/MadryLab/mnist_challenge, May 2019.
- [55] N. Papernot, P. D. McDaniel, and I. J. Goodfellow, "Transferability in machine learning: from phenomena to black-box attacks using adversarial samples," *CoRR*, vol. abs/1605.07277, 2016.
- [56] T. Salimans, J. Ho, X. Chen, and I. Sutskever, "Evolution strategies as a scalable alternative to reinforcement learning," *CoRR*, vol. abs/1703.03864, 2017. [Online]. Available: <http://arxiv.org/abs/1703.03864>
- [57] D. Wierstra, T. Schaul, T. Glasmachers, Y. Sun, J. Peters, and J. Schmidhuber, "Natural evolution strategies," *Journal of Machine Learning Research*, vol. 15, no. 1, pp. 949–980, 2014.
- [58] P. Zhao, S. Liu, P. Chen, N. Hoang, K. Xu, B. Kailkhura, and X. Lin, "On the design of black-box adversarial examples by leveraging gradient-free optimization and operator splitting method," in *ICCV 2019 (accepted)*, 2019.
- [59] J. Su, D. V. Vargas, and K. Sakurai, "One pixel attack for fooling deep neural networks," *IEEE Transactions on Evolutionary Computation*, 2019.
- [60] W. Xu, Y. Qi, and D. Evans, "Automatically evading classifiers: A case study on pdf malware classifiers," in *Proceedings of the 2016 Network and Distributed Systems Symposium*, 2016, pp. 21–24.
- [61] K. T. Co, L. Muñoz-González, S. de Maupéou, and E. C. Lupu, "Procedural noise adversarial examples for black-box attacks on deep convolutional networks," in *CCS 2019 (accepted)*, 2019.
- [62] J. Lu, H. Sibai, and E. Fabry, "Adversarial examples that fool detectors," *CoRR*, vol. abs/1712.02494, 2017.
- [63] S. T. K. Jan, J. Messou, Y. Lin, J. Huang, and G. Wang, "Connecting the digital and physical world: Improving the robustness of adversarial attacks," in *The Thirty-Third AAAI Conference on Artificial Intelligence*, 2019, pp. 962–969.
- [64] K. Eykholt, I. Evtimov, E. Fernandes, B. Li, D. Song, T. Kohno, A. Rahmati, A. Prakash, and F. Tramèr, "Note on attacking object detectors with adversarial stickers," *CoRR*, vol. abs/1712.08062, 2017.
- [65] T. B. Brown, D. Mané, A. Roy, M. Abadi, and J. Gilmer, "Adversarial patch," *CoRR*, vol. abs/1712.09665, 2017.
- [66] J. Lu, H. Sibai, E. Fabry, and D. A. Forsyth, "NO need to worry about adversarial examples in object detection in autonomous vehicles," *CoRR*, vol. abs/1707.03501, 2017.
- [67] C. Sitawarin, A. N. Bhagoji, A. Mosenia, M. Chiang, and P. Mittal, "DARTS: deceiving autonomous cars with toxic signs," *CoRR*, vol. abs/1802.06430, 2018.
- [68] S.-T. Chen, C. Cornelius, J. Martin, and D. H. Chau, "Shapeshifter: Robust physical adversarial attack on faster r-cnn object detector," *ArXiv*, vol. abs/1804.05810, 2018.
- [69] K. Eykholt, I. Evtimov, E. Fernandes, B. Li, A. Rahmati, F. Tramèr, A. Prakash, T. Kohno, and D. Song, "Physical adversarial examples for object detectors," in *12th USENIX Workshop on Offensive Technologies*, 2018.
- [70] D. Maiorca, I. Corona, and G. Giacinto, "Looking at the bag is not enough to find the bomb: an evasion of structural methods for malicious pdf files detection," in *Proceedings of the 8th ACM SIGSAC symposium on Information, computer and communications security*. ACM, 2013, pp. 119–130.
- [71] N. Srndic and P. Laskov, "Practical evasion of a learning-based classifier: A case study," in *2014 IEEE Symposium on Security and Privacy*, 2014, pp. 197–211.
- [72] K. Grosse, N. Papernot, P. Manoharan, M. Backes, and P. McDaniel, "Adversarial examples for malware detection," in *European Symposium on Research in Computer Security*. Springer, 2017, pp. 62–79.
- [73] A. Demontis, M. Melis, B. Biggio, D. Maiorca, D. Arp, K. Rieck, I. Corona, G. Giacinto, and F. Roli, "Yes, machine learning can be more secure! a case study on android malware detection," *IEEE Transactions on Dependable and Secure Computing*, 2017.
- [74] L. Xu, Z. Zhan, S. Xu, and K. Ye, "An evasion and counter-evasion study in malicious websites detection," in *IEEE Conference on Communications and Network Security*. IEEE, 2014, pp. 265–273.
- [75] D. Lowd and C. Meek, "Good word attacks on statistical spam filters," in *CEAS*, vol. 2005, 2005.
- [76] X. Yuan, Y. Chen, Y. Zhao, Y. Long, X. Liu, K. Chen, S. Zhang, H. Huang, X. Wang, and C. A. Gunter, "Commandersong: A systematic approach for practical adversarial voice recognition," in *27th USENIX Security Symposium, USENIX Security*, 2018, pp. 49–64.
- [77] N. Carlini, P. Mishra, T. Vaidya, Y. Zhang, M. Sherr, C. Shields, D. A. Wagner, and W. Zhou, "Hidden voice commands," in *25th USENIX Security Symposium*, 2016, pp. 513–530.
- [78] F. Chollet *et al.*, "Keras," <https://keras.io>, 2015.
- [79] A. Madry, A. Makelov, L. Schmidt, D. Tsipras, and A. Vladu, "Towards deep learning models resistant to adversarial attacks," in *Proceedings of International Conference on Learning Representations*, 2018.
- [80] Y. Dong, F. Liao, T. Pang, H. Su, J. Zhu, X. Hu, and J. Li, "Boosting adversarial attacks with momentum," in *Proceedings of 2018 IEEE Conference on Computer Vision and Pattern Recognition*, 2018, pp. 9185–9193.
- [81] W. He, B. Li, and D. Song, "Decision boundary analysis of adversarial examples," in *Proceedings of International Conference on Learning Representations*, 2018.
- [82] P. Chen, Y. Sharma, H. Zhang, J. Yi, and C. Hsieh, "EAD: elastic-net attacks to deep neural networks via adversarial examples," in *Proceedings of the Thirty-Second AAAI Conference on Artificial Intelligence (AAAI)*, 2018, pp. 10–17.
- [83] S. Moosavi-Dezfooli, A. Fawzi, and P. Frossard, "Deepfool: A simple and accurate method to fool deep neural networks," in *Proceedings of 2016 IEEE Conference on Computer Vision and Pattern Recognition*, 2016, pp. 2574–2582.
- [84] Y. Sun, X. Huang, and D. Kroening, "Testing deep neural networks," *CoRR*, vol. abs/1803.04792, 2018.
- [85] Y. Sun, M. Wu, W. Ruan, X. Huang, M. Kwiatkowska, and D. Kroening, "Concolic testing for deep neural networks," in *Proceedings of the 33rd ACM/IEEE International Conference on Automated Software Engineering*, 2018, pp. 109–119.
- [86] O. Bastani, Y. Ioannou, L. Lampropoulos, D. Vytiniotis, A. V. Nori, and A. Criminisi, "Measuring neural net robustness with constraints," in *NIPS*, 2016, pp. 2613–2621.
- [87] X. Huang, M. Kwiatkowska, S. Wang, and M. Wu, "Safety verification of deep neural networks," in *Proceedings of the 29th International Conference on Computer Aided Verification*, 2017, pp. 3–29.
- [88] R. Ehlers, "Formal verification of piece-wise linear feed-forward neural networks," in *Proceedings of the 15th International Symposium on Automated Technology for Verification and Analysis*, 2017, pp. 269–286.
- [89] V. Tjeng, K. Xiao, and R. Tedrake, "Evaluating robustness of neural networks with mixed integer programming," 2019.
- [90] W. Ruan, X. Huang, and M. Kwiatkowska, "Reachability analysis of deep neural networks with provable guarantees," in *Proceedings of the Twenty-Seventh International Joint Conference on Artificial Intelligence*, 2018, pp. 2651–2659.

- [91] S. Wang, K. Pei, J. Whitehouse, J. Yang, and S. Jana, "Formal security analysis of neural networks using symbolic intervals," in *Proceedings of the 27th USENIX Security Symposium on Security*, 2018, pp. 1599–1614.
- [92] K. Dvijotham, R. Stanforth, S. Gowal, T. A. Mann, and P. Kohli, "A dual approach to scalable verification of deep networks," *CoRR*, vol. abs/1803.06567, 2018.
- [93] <https://github.com/peikexin9/deeplxplore/issues/20>.
- [94] <https://github.com/bethgelab/foolbox/issues/264>.
- [95] <https://github.com/tensorflow/cleverhans/issues/265>.
- [96] P. Tabacof and E. Valle, "Exploring the space of adversarial images," in *2016 International Joint Conference on Neural Networks, IJCNN 2016, Vancouver, BC, Canada, July 24-29, 2016*. IEEE, 2016, pp. 426–433. [Online]. Available: <https://doi.org/10.1109/IJCNN.2016.7727230>
- [97] J. Rauber, W. Brendel, and M. Bethge, "Foolbox: A python toolbox to benchmark the robustness of machine learning models," *arXiv preprint arXiv:1707.04131*, 2017.
- [98] W. Brendel, J. Rauber, M. Kümmerer, I. Ustuzhaninov, and M. Bethge, "Accurate, reliable and fast robustness evaluation," *CoRR*, vol. abs/1907.01003, 2019.
- [99] Y. Shi, S. Wang, and Y. Han, "Curls & whey: Boosting black-box adversarial attacks," in *Computer Vision and Pattern Recognition (CVPR), 2019*, 2019.
- [100] Y. Yu, H. Qian, and Y.-Q. Hu, "Derivative-free optimization via classification," in *Thirtieth AAAI Conference on Artificial Intelligence*, 2016.
- [101] J. Sekhon and C. Fleming, "Towards improved testing for deep learning," in *Proceedings of the 41st International Conference on Software Engineering: New Ideas and Emerging Results (ICSE)*, 2019, pp. 85–88.
- [102] J. Guo, Y. Jiang, Y. Zhao, Q. Chen, and J. Sun, "Dlfuzz: differential fuzzing testing of deep learning systems," in *Proceedings of the 2018 ACM Joint Meeting on European Software Engineering Conference and Symposium on the Foundations of Software Engineering (ESEC/SIGSOFT)*, 2018, pp. 739–743.
- [103] X. Xie, L. Ma, F. Juefei-Xu, M. Xue, H. Chen, Y. Liu, J. Zhao, B. Li, J. Yin, and S. See, "Deephunter: a coverage-guided fuzz testing framework for deep neural networks," in *Proceedings of the 28th ACM SIGSOFT International Symposium on Software Testing and Analysis (ISSTA)*, 2019, pp. 146–157.
- [104] A. Kurakin, I. J. Goodfellow, and S. Bengio, "Adversarial machine learning at scale," in *Proceedings of the 5th International Conference on Learning Representations (ICLR)*, 2017.
- [105] K. He, X. Zhang, S. Ren, and J. Sun, "Deep residual learning for image recognition," in *2016 IEEE Conference on Computer Vision and Pattern Recognition (CVPR)*, 2016, pp. 770–778.
- [106] G. Huang, Z. Liu, L. van der Maaten, and K. Q. Weinberger, "Densely connected convolutional networks," in *2017 IEEE Conference on Computer Vision and Pattern Recognition*, 2017, pp. 2261–2269.
- [107] I. J. Goodfellow, D. Warde-Farley, M. Mirza, A. C. Courville, and Y. Bengio, "Maxout networks," in *Proceedings of the 30th International Conference on Machine Learning*, 2013, pp. 1319–1327.
- [108] A. Coates, A. Y. Ng, and H. Lee, "An analysis of single-layer networks in unsupervised feature learning," in *Proceedings of the Fourteenth International Conference on Artificial Intelligence and Statistics*, 2011, pp. 215–223.

APPENDIX

A. Discussion on Normalization

In this section, we first survey several typical normalization and then discuss why it is non-trivial to infer the normalization in black-box scenario.

Computer vision usually require some normalization (also known as preprocessing) because the original input comes in a form that is difficult for many deep learning architectures to represent. The images should be normalized so that their pixels all lie in the same, reasonable range, like $[0, 1]$ or $[-1, 1]$ or $[-0.5, 0.5]$. Mixing images that lie different ranges will usually result in failure [45].

Dataset augmentation is a kind of preprocessing for the training set only. Other kinds of normalization are applied

to both the train and the test sets with the goal of putting each example into a more canonical form in order to reduce the amount of variation that the model needs to account for. Therefore, in this section, we only discuss normalization for test set. We do not consider size-normalization, i.e., normalizing images into same size, which would make inference more difficult. Specifically, we will present several widely used approaches for normalizing images into some range.

1) *Normalization for MNIST Images*: The original MNIST images are black and white images and the resulting images are grayscale images as a result of the anti-aliasing technique used by the normalization algorithm. Each pixel of a grayscale image has only one channel whose value is an integer ranging from 0 to 255, where 0 means background (white), 255 means foreground (black). For classification of handwritten digits, the value of each pixel is usually normalized into the range $[0, 1]$ by dividing 255.

2) *Normalization for ImageNet Images*: The ImageNet images are represented in red, green and blue colors, then, each pixel of an ImageNet image has three channels. The value of each channel is an integer ranging from 0 to 255. We list three different normalization below.

- **The Inception-v3 model in ZOO [30]**: the integer value i of each channel is normalized into a real value r as follows:

$$r = \frac{i}{255} - 0.5.$$

Obviously, the range of r is $[-0.5, 0.5]$.

- **The Inception-v3 model in Keras [78]**: the integer value i of each channel is normalized into a real value r as follows:

$$r = \frac{2 \times i}{255} - 1.$$

Obviously, the range of r is $[-1, 1]$.

- **The VGG and ResNet models in Keras [78]**: the integer value i of each channel j ($j = 1, 2, 3$) is normalized into a real value r as follows:

$$r = i - \text{mean}_j$$

where $\text{mean}_j = \frac{\sum_{d \in \text{TDS}} \sum_{(w,h,j) \in P} d[w,h,j]}{\frac{|P|}{3} \times |\text{TDS}|}$, and TDS denotes the training dataset. Recall that P denotes the set of coordinates. Obviously, the range of r is $[-255, 255]$ and depends on the training dataset.

- **The DenseNet model in [106] and ResNet model in torch**²: the integer value i of each channel j is normalized into a real value r as follows:

$$r = \frac{i - \text{mean}_j}{\text{std}_j}$$

where mean_j is defined the same as above, the standard deviation std_j is defined as follows:

$$\text{std}_j = \sqrt{\frac{\sum_{d \in \text{TDS}} \sum_{(w,h,j) \in P} (d[w,h,j] - \text{mean}_j)^2}{\frac{|P|}{3} \times |\text{TDS}|}}.$$

²<https://github.com/facebook/fb.resnet.torch>

Obviously, the range of r is $[-\infty, \infty]$ and depends on the training dataset.

3) *Normalization for CIFAR-10 Images:*

- **The DenseNet model in [106]:** the integer value i of each channel j is normalized into a real value r as follows:

$$r = \frac{i - \text{mean}_j}{\text{std}_j}$$

where mean_j and std_j are defined the same as above. Then, the range of r is $[-\infty, \infty]$ and depends on the training dataset.

- **The maxout model in [107] (cf. [45, Page 472]):** the integer value i of each channel j is normalized into a real value r as follows:

$$r = s \times \frac{i - \text{mean}_j}{\max\{10^{-8}, \text{std}_j\}}$$

where mean_j and std_j are defined the same as above. The extremely low value 10^{-8} is introduced to avoid division by 0. The scale parameter s is chosen to make each individual pixel have standard deviation across examples close to 1. The range of r depends on s and dataset.

- **The model in [108] (cf. [45, Page 472]):** the integer value i of each channel j is normalized into a real value r as follows:

$$r = \frac{i - \text{mean}_j}{\text{std}'_j}$$

where mean_j is defined the same as above and std'_j is defined as follows:

$$\text{std}'_j = \sqrt{10 + \frac{\sum_{d \in \text{TDS}} \sum_{(w,h,j) \in P} (d[w, h, j] - \text{mean}_j)^2}{\frac{|P|}{3} \times |\text{TDS}|}}$$

The range of r is $[-\frac{255}{\sqrt{10}}, \frac{255}{\sqrt{10}}]$ and depends on the training dataset. Note that 10 is introduced to avoid division by 0

4) *Discussion:* As shown above, we can observe that: (1) the same network model on the same dataset (e.g., Inception-v3 and ResNet models on ImageNet images) in different tools may use different normalization; (2) the same tool may use different normalization for different models even on the same dataset (e.g., Inception-v3 and ResNet in Keras on ImageNet); and (3) there are several kinds of normalization and the parameters of normalization may depend on training dataset. Once the normalization is known, its corresponding denormalization can be implemented by choosing a rounding mechanism, e.g., round up, round down, round to the nearest integer. In black-box scenario, the adversary can only query discrete integer images to the oracle classifier and get the output, without the knowledge of training dataset, architecture, parameters and normalization of the classifier. To our knowledge, in general, it is non-trivial to infer how the normalization is implemented by a classifier.

B. Results of Parameter Tuning

Strategy S1 aims at controlling perturbation step sizes. Among 9 tools, NES-PGD, DBA, Bandits and GenAttack provide such adaptive mechanism. We limit the L_∞ distance

at discrete domain firstly, then constraint the perturbation step sizes as integer numbers. e.g., the parameters α in NES-PGD, ‘step adaption’ in DBA and ‘adaptive’ in GenAttack. Using this strategy, the TSR of NES-PGD and DBA increases, but the TSR of Bandits and GenAttack does not increases (cf. Section IV-B for reasons). The results are shown in Table X. We can observe that the TSR of NES-PGD increases at the cost of higher query times, due to the fact that limiting of the dynamic adjustment of step size or learning rate, will affect the attack efficiency of this method.

TABLE X
PARAMETERS AND RESULTS OF S1

NES-PGD [37] attack on ImageNet+InceptionV3					
Version1 (default): $\epsilon = 0.05, \alpha \in [1e-2, 5e-5]$					
Version2: $\epsilon = 10/255, \alpha \in [1e-2, 5e-5]$					
Version3: $\epsilon = 10/255, \alpha = 1/255$					
Version	SR	TSR	MSE	Discr. Error	Avg. Queries
1	100%	53%	8.77e-04	≈ 0.5	12470
2	100%	47%	5.46e-04	≈ 0.5	16168
3	74%	73%	5.14e-04	0.16	214552

DBA [24] attack on ImageNet+VGG19					
Version1 (baseline): iteration = 1000, $\alpha = 0.01$, step adaptation = 1.5					
Version2: iteration = 1000, $\alpha = 1/255$, step adaptation = 1					
Version	SR	TSR	MSE	Discr. Error	
1	100%	51%	3.56e-04	≈ 0.5	
2	100%	62%	0.016	≈ 0.5	

Bandits [50] attack on ImageNet+InceptionV3					
Version1 (default): $\epsilon = 0.05, \alpha = 0.01$					
Version2: $\epsilon = 10/255, \alpha = 0.01$					
Version3: $\epsilon = 10/255, \alpha = 1/255$					
Version	SR	TSR	MSE	Discr. Error	Avg. Queries
1	94%	11%	2.08e-03	≈ 0.5	2715
2	92%	12%	1.4e-03	≈ 0.5	2923
3	92%	11%	1.23e-03	≈ 0.5	2950

GenAttack [51] attack on ImageNet+InceptionV3					
Version1 (default): $\epsilon = 0.05, \alpha \approx 0.15$, adaptive=True					
Version2: $\epsilon = 10/255, \alpha \approx 0.1$, adaptive=True					
Version3: $\epsilon = 10/255, \alpha = 0.1$, adaptive=False					
Version	SR	TSR	MSE	Discr. Error	Avg. Queries
1	100%	91%	1.61e-03	≈ 0.5	24728
2	97%	56%	1.05e-03	≈ 0.5	33273
3	99%	46%	4.39e-04	≈ 0.5	45576

Strategy S2 aims at minimizing the ratio of discretization error against the overall perturbations. L-BFGS, DeepFool, DeepXplore and DBA provide input parameters related to this strategy. For L-BFGS, we increase ‘initial const’, which could relax the distance constraint, and reduce the binary search which could also avoid constraint enhancement. For DeepFool, ‘overshot’ controls the distance cross polyhedral boundary, as same as DeepXplore, ‘step’ multiplies with gradient to get the perturbation. For DBA, since adversarial examples are starting from target images, if we reduce ‘iteration’, the distance between adversarial and original image will be reduced. Experimental results show that the TSR of DBA can increase at the cost of higher overall perturbations, but the TSR of L-BFGS, DeepFool and DeepXplore does not increase obviously.

TABLE XI
PARAMETERS AND RESULTS OF THE S2

L-BFGS [13] attack on ImageNet+Inception-v3				
Version1 (default): initial const = 1e-2, binary search steps = 5				
Version2: initial const = 1e-2, binary search steps = 3				
Version3: initial const = 5e-2, binary search steps = 3				
Version	SR	TSR	MSE	Discr. Error
1	100%	77%	2.27e-05	≈ 0.5
2	100%	76%	2.29e-05	≈ 0.5
3	100%	79%	4.29e-05	≈ 0.5

DeepFool [83] attack on ImageNet+ResNet34				
Overshoot	SR	TSR	MSE	Discr. Error
1.02	100%	23%	2.27e-05	≈ 0.5
1.5	100%	23%	3.79e-05	≈ 0.5
2	100%	24%	6.16e-05	≈ 0.5

DeepXplore [22] attack on ImageNet+ResNet50&VGG16&19				
Version1 (default): weight diff=1, step=10				
Version2: weight diff=1, step=20				
Version3: weight diff=2, step=10				
Version	SR	TSR	MSE	Discr. Error
1	65%	28%	2.14e-02	≈ 0.5
2	64%	25%	2.25e-02	≈ 0.5
3	65%	29%	2.22e-02	≈ 0.5

DBA [24] attack on ImageNet+VGG19				
Version1 (default): iteration = 5000, $\alpha = 0.01$, step adaptation = 1.5				
Version2: iteration = 1000, $\alpha = 0.01$, step adaptation = 1.5				
Version	SR	TSR	MSE	Discr. Error
1	100%	28%	1.91e-05	≈ 0.5
2	100%	51%	3.56e-04	≈ 0.5

Strategy S3 aims at enhancing the robustness of real adversarial samples against the discretization problem. Both C&W and ZOO provide such input parameters (i.e., κ). The results are shown in Table XII. We can observe that the TSR of C&W increase at the cost of higher overall perturbations (cf. mean-square error (MSE) in Table XII). However, it does not work for ZOO, although ZOO is a black box version of C&W by leveraging gradient estimation. This is because that ZOO fails to find adversarial samples when the confidence constraint κ increasing.

TABLE XII
PARAMETERS AND RESULTS OF THE S3

C&W-L ₂ [18] attack on ImageNet+InceptionV3				
κ	SR	TSR	MSE	Discr. Error
0	100%	10%	1.51e-06	≈ 0.5
15	100%	99%	5.88e-06	≈ 0.5
30	100%	100%	1.27e-05	≈ 0.5

ZOO [30] attack on ImageNet+Inception-v3				
κ	SR	TSR	MSE	Discr. Error
0	58%	6%	1.07e-05	≈ 0.5
15	0%	-	-	-
30	0%	-	-	-

For greedy search based version of C&W, the problem of searching adversarial examples is reduced to the solving of the following optimization problem:

$$\text{minimize } c \times f(x + \delta) + \|\delta\|_2$$

where c is an input parameter, f is a loss function, x is the original image, and δ is the perturbation. We tune the input parameter c (i.e., init const in their implementation) and the number of iterations of the binary search which is used to minimize distortion once an adversarial example is found. These fine-tuned parameters could improve TSR well after combining with greedy search..

TABLE XIII
PARAMETERS AND RESULTS OF THE GREEDY SEARCH BASED VERSION OF C&W

C&W-L ₂ [18] attack on MNIST+original model				
Version1 (default): init const=1e-3, binary search=9, no greedy search				
Version2: init const=1e-3, binary search=9, greedy search				
Version3: init const=1, binary search=3, no greedy search				
Version4: init const=1, binary search=3, greedy search				
Version	SR	TSR	MSE	Search steps
1	100%	22.89%	4.57e-03	N/A
2	100%	99.67%	4.6e-03	$\infty(200000)$
3	100%	60%	4.54e-03	N/A
4	100%	100%	4.56e-03	237